SLAC-PUB-2605
September 1980
(T/E)

EXCLUSIVE PROCESSES AND HADRON DYNAMICS AT SHORT DISTANCES*

Stanley J. Brodsky
Stanford Linear Accelerator Center
Stanford University, Stanford, California 94305

and

G. Peter Lepage†
Laboratory of Nuclear Studies
Cornell University, Ithaca, New York 14853

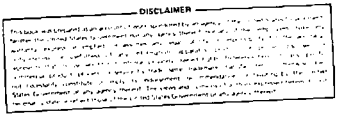

(Invited talk presented at the XI International Symposium on Multiparticle Dynamics, Bruges, Belgium, June 22-27, 1980.)

and

(The Symposium on Topical Questions in QCD, Copenhagen, Denmark, June 9-13, 1980.)

* Work supported by the Department of Energy, contract DE-AC03-76SF00515.
† Work supported by the National Science Foundation.

Abstract

Exclusive processes and hadron dynamics at short distances by S. J. Brodsky (Stanford Linear Accelerator Center, Stanford University, Stanford, California 94305) and G. P. Lepage (Laboratory of Nuclear Studies, Cornell University, Ithaca, New York 14853).

The predictions of perturbative QCD for a number of areas of hadron dynamics are discussed, including exclusive processes at large momentum transfer, the endpoint behavior of hadronic structure functions, and the Fock state structure of hadron wavefunctions -- especially their behavior at short-distance. New results for exclusive two-photon processes, the normalization of high twist contributions to the meson structure function, and the calculation of the valence Fock state probability of the pion are presented. We also review the contrasting features of QCD and parton model dynamics.

1. Introduction

One of the most important areas of applications of quantum chromodynamics is the study of hadron dynamics at short distances. As we have discussed in a series of recent papers [1-6], large momentum transfer exclusive processes and the short distance structure of hadronic wavefunctions can be systematically analyzed within the context of perturbative quantum chromodynamics [7]. The analysis provides a systematic method for calculating elastic and inelastic form factors and the hard-scattering contributions which dominate fixed-angle hadronic scattering amplitudes as a perturbation expansion in the QCD running coupling constant, α_s. Many of the predictions such as those for the meson form factors [8,9], two-photon processes $\gamma\gamma \to M\bar{M}$ [5], and the structure of the hadron wavefunctions at large momentum transfer are derived at the same level of rigor as the QCD predictions for the structure function moments and the annihilation ratio $\sigma(e^+e^- \to X)/\sigma(e^+e^- \to \mu^+\mu^-)$.

Thus far, the most extensive efforts in testing perturbative QCD have been concentrated in the area of inclusive reactions. In the case of deep inelastic lepton scattering, lepton-pair production, and e^+e^- annihilation cross sections, the basic scale-invariance of QCD is revealed through logarithmic modifications of QED or weak interaction amplitudes which must be verified over a large range of kinematics. Direct checks of the coupling of QCD at the Born level are possible in inclusive reactions such as e^+e^- annihilation into three or more jets, and the production of hadrons, jets, or photons at very large transverse momenta in hadron-hadron collisions.

As we shall discuss here, large momentum transfer exclusive reactions provide an extensive, experimentally accessible, and perhaps definitive testing ground for perturbative QCD. In particular, the power-law behavior of these reactions directly tests the scale-invariance of the basic quark and gluon interactions at short distances, as well as the SU(3)-color symmetry of the hadronic valence wavefunctions. The normalizations of the

exclusive amplitudes (both relative and absolute) test the basic flavor and spin symmetry structure of the theory as well as the asymptotic boundary condition for meson valence state wavefunctions obtained from the meson leptonic decay rates. The angular variation, helicity structure, and absolute sign of exclusive amplitudes test the spin and bare couplings of quarks and gluons. In addition the predicted logarithmic modifications of exclusive amplitudes reflect the asymptotic freedom variation of the running coupling constant and the singularities in the operator product expansion of hadronic wave functions at short distances [1,2]. In particular, the process-independent distribution amplitudes $\phi(x_i,Q)$ (which specify the longitudinal momentum distributions for valence quarks collinear up to the scale Q) have a logarithmic dependence in Q which is completely determined by QCD evolution equations, or equivalently, by the operator product expansion of the hadronic Bethe-Salpeter wavefunction near the light-cone. The large transverse momentum tail of the hadronic wave functions $\psi(x_i,k_{\perp i})$ is thus calculable in perturbative QCD; we emphasize that (modulo calculable logarithms), $\psi(x_i,k_{\perp i})$ falls only as $1/k_{\perp i}^2$ at large quark transverse momenta — not exponentially as is often assumed in phenomenological applications.

The underlying link between different hadronic phenomenon in quantum chromodynamics is the hadronic wavefunction. Many features of the Fock state wavefunctions in QCD are quite different from that which had been expected in the parton model. We will define [11] the states at equal time $\tau = t+z$ on light-cone in the light-cone gauge $A^+ = A^0 + A^3 = 0$. The amplitude to find n (on-mass-shell) quarks and gluons in a hadron with 4-momentum P directed along the Z-direction and spin projection S_z is defined ($k^\pm = k^0 \pm k^3$) (see Fig. 1)

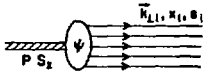

Fig. 1. The amplitude to find n (on-mass-shell) quarks and gluons in a hadron.

$$\psi^{(n)}_{S_z}(x_i, \vec{k}_{\perp i}, s_i) \quad , \quad x_i \equiv \frac{k_i^+}{P^+} \quad ,$$

where by momentum conservation $\sum_{i=1}^{n} x_i = 1$ and $\sum_{i=1}^{n} \vec{k}_{\perp i} = 0$. The s_i specify the the spin-projection of the constituents. The state is off the light-cone energy shell,

$$P^- - \sum_{i=1}^{n} k_i^- = \frac{M^2 - \sum_{i=1}^{n} \frac{\vec{k}^2_{\perp i} + m_i^2}{x_i}}{P^+} < 0 \quad . \qquad (1.1)$$

The valence Fock states (which in fact dominate large momentum transfer exclusive reactions) are the $|q\bar{q}\rangle$ $(n = 2)$ and $|qqq\rangle$ $(n = 3)$ components of the meson and baryon. For each fermion or anti-fermion constituent $\psi^{(n)}_{S_z}(k_{\perp i}, x_i, s_i)$ multiplies the spin factor $u(\vec{k}_i)/\sqrt{k_i^+}$ or $v(\vec{k}_i)/\sqrt{k_i^+}$. The wavefunction normalization condition is

$$\sum_{(n)(s_i)} \int \left|\psi^{(n)}_{S_z}(k_{\perp i}, x_i, s_i)\right|^2 [d^2k_\perp][dx] = 1 \quad , \qquad (1.2)$$

where

$$[d^2k_\perp] \equiv 16\pi^3 \delta^{(2)}\left(\sum_i k_{\perp i}\right) \prod_{i=1}^{n} \frac{d^2k_{\perp i}}{16\pi^3} \quad ,$$

and

$$[dx] = \delta\left(1 - \sum_i x_i\right) \prod_{i=1}^{n} dx_i \quad .$$

By studying the wavefunctions themselves, one could in principle understand not only the origin of the standard structure functions, but also the nature of multi-particle longitudinal and transverse momentum distributions, helicity dependences, as well as the effects of coherence. For example, the standard quark and gluon structure functions (probability distributions) which control large momentum transfer inclusive reactions at the scale Q^2 are

$$G_{a/H}(x_a,Q^2) \equiv d_a^{-1}(Q^2) \sum_{n,s_i,s_z} \int^{k_{1a}^2 < Q^2} \left|\psi^{(n)}_{s_z}(k_{1i},x_i,s_i)\right|^2 [d^2k_i][dx]\,\delta(x-x_a) \ , \tag{1.3}$$

where $d_a^{-1}(Q^2)$ is due to the wavefunction renormalization of the constituent a. Note that only terms which fall-off as $|\psi|^2 \sim (k_{1a}^2)^{-1}$ (modulo logs) contribute to the Q^2 dependence of the integral. These contributions are analyzable by the renormalization group and correspond in perturbative QCD to quark or gluon pair production or fragmentation processes associated with the struck constituent a. In general, unless x is close to 1, all Fock states in the hadron contribute to $G_{a/H}$. Multi-particle probability distributions are simple generalizations of Eq. (1.3).

Inclusive cross sections in QCD are then obtained by a summation over incoherent hard-scattering subprocess cross sections:

$$d\sigma_{AB\to CX} = \sum_i \int_0^1 dx_a \int_0^1 dx_b\, G_{a/A}(x_a,\tilde{Q})\, G_{b/B}(x_b,\tilde{Q})\, d\hat{\sigma}^i_{ab\to X} \tag{1.4}$$

where each subprocess $d\hat{\sigma}$ is computed for on-shell constituents a and b which are collinear with A and B. This result is obtained by integrating the hadronic wavefunctions up to the momentum transfer scale Q; the exact definition of $\tilde{Q}$ is discussed in Sect. 4. The correct prescription for including k_T fluctuations from the wavefunctions is to sum over higher-twist subprocesses $d\sigma_{ab}$ where a and b are each clusters of quarks and gluons in the Fock state wavefunctions. The hard-scattering summation procedure [12] handles the off-shell kinematics of the constituents correctly and can done in a well-defined gauge-invariant manner. The naive procedure of smearing the leading twist cross section leads to infinite results (in the case of gluon-exchange processes) and cannot be justified in QCD.

Exclusive reactions at large transverse momentum can also be written in a form which factorizes the dynamics of the hard-scattering processes from the physics of the hadronic wavefunctions. A simple picture emerges from

our analysis of these processes. For example, consider the proton's magnetic form factor, $G_M(Q^2)$, at large $-q^2 = Q^2$. This is most easily understood in the infinite momentum frame where the proton is initially moving along the z-axis and then is struck by a highly virtual photon carrying large transverse momentum $q_\perp^2 = -q^2$. The form factor is the amplitude for the composite hadron to absorb large transverse momentum while remaining intact. In effect, an "intact" baryon can be pictured as three valence quarks, each carrying some fraction x_i of the baryon's momentum $\left(\sum_{i=1}^{3} x_i = 1\right)$ and all moving roughly parallel with the hadron. As we shall see, the more complicated non-valence Fock states in the proton (i.e., $qqqq\bar{q}$,$qqqg$,...) are unimportant as $Q^2 \to \infty$. The form factor is then the product of three probability amplitudes: (a) the amplitude, ϕ, for finding the three-quark valence state in the incoming proton; (b) the amplitude, T_H, for this quark state to scatter with the photon producing three quarks in the final state whose momenta are roughly collinear; and (c) the amplitude, ϕ^*, for this final quark state to reform into a hadron. Thus the magnetic form factor can be written (see Fig. 2a) [1,2]

$$G_M(Q^2) = \int_0^1 [dx] \int_0^1 [dy]\, \phi^*(y_i, \tilde{Q}_y)\, T_H(x_i, y_i, Q)\, \phi(x_i, \tilde{Q}_x)\left[1 + \mathcal{O}(m^2/Q^2)\right] \quad (1.5)$$

where $\tilde{Q}_x \equiv \min_i (x_i Q)$.

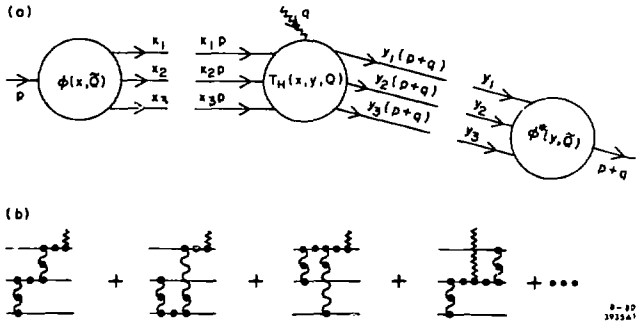

Fig. 2. (a) The general factorized structure of the nucleon form factor at large Q^2 in QCD. (b) Leading contributions to the hard-scattering amplitude T_H.

To leading order in $\alpha_s(Q^2)$, the "hard-scattering amplitude" T_H is the sum of all Born diagrams for $\gamma^* + 3q \to 3q$ in perturbative QCD [see Fig. 2b]. The transverse momentum fluctuations of the quarks in the initial and final protons are negligible relative to $q_\perp$, as are all particle masses. These can be ignored in T_H so that in effect each hadron is replaced by collinear on-shell valence partons. Since the final quarks are collinear, momentum of $\mathcal{O}(q_\perp) \to \infty$ must be transferred from quark line to quark line (via gluons) in T_H. This justifies our use of perturbation theory in computing T_H, since all internal propagators in the Born diagrams must then be off-shell by $\mathcal{O}(Q^2)$. Furthermore the most important dynamical feature of the form factor -- its power-law fall-off -- can then be traced to the behavior of T_H, which falls for increasing Q^2 with a factor $\left(\alpha_s(Q^2)/Q^2\right)$ for each constituent, after the first, scattered from the incident to the final direction: i.e.,

$$T_H\left(x_i, y_i, Q\right) = \left(\frac{\alpha_s(Q^2)}{Q^2}\right)^2 T\left(x_i, y_i\right)\left[1 + \mathcal{O}\left(\alpha_s(Q^2)\right)\right] \qquad (1.6)$$

where $\alpha_s(Q^2) = (4\pi/\beta)(\ell n\, Q^2/\Lambda^2)^{-1}$ is the running coupling constant.

It is now clear that non-valence Fock states in the proton cannot contribute since all such states contain four or more constituents, each of which must be turned to the final direction. Thus T_H for these states falls as $\left(\alpha_s(Q^2)/Q^2\right)^3$ or faster and is negligible relative to (1.6) as $Q^2 \to \infty$. [This observation, while strictly true in light-cone gauge ($n\cdot A = A^+ = 0$), has a different interpretation in covariant gauges.] Thus non-valence ("sea") quarks and gluons in the proton do not contribute. The quantity $\phi(x,Q)$ is the "distribution amplitude" for finding the valence quark with light-cone fraction x_i in the hadron at relative separation $b_\perp \sim \mathcal{O}(1/Q)$. In fact [1,2],

$$\phi(x_i, s_i, Q) \equiv \prod_{i=1}^{n}\left[d_i^{-1}(Q^2)\right]^{\frac{1}{2}} \int^{k_{1i}^2 < Q^2} [d^2k_\perp]\, \psi^{(n)}\left(k_{1i}, x_i, s_i\right). \qquad (1.7)$$

This amplitude is obviously process independent. It contains the essential physics of that part of the hadronic wavefunction which affects exclusive

processes with large momentum transfer. The distribution amplitude is only weakly dependent on Q^2, and this dependence is completely specified by an evolution equation of the form (in leading order)

$$Q^2 \frac{\partial}{\partial Q^2} \phi(x_i,Q) = \frac{\alpha_s(Q^2)}{4\pi} \int_0^1 [dy]\ V(x_i,y_i)\phi(y_i,Q) \qquad (1.8)$$

where V can be computed from a single gluon exchange kernel. The general solution of this equation is

$$\phi(x_i,Q) = x_1x_2x_3 \sum_{n=0}^{\infty} a_n \left(\ell n\ \frac{Q^2}{\Lambda^2}\right)^{-\gamma_n} \tilde{\phi}_n(x_i) \quad . \qquad (1.9)$$

Combining this expansion with Eqs. (1.5) and (1.6), we obtain the general form of G_M:

$$G_M(Q^2) = \left(\frac{\alpha_s(Q^2)}{Q^2}\right)^2 \sum_{n,m} b_{nm} \left(\ell n\ \frac{Q^2}{\Lambda^2}\right)^{-\gamma_n-\gamma_m} \quad . \qquad (1.10)$$

The factorized form of Eq. (1.5) implies a simple space-time picture. The exchange of large transverse momentum in the hard-scattering amplitude T_H occurs only when the relative separation of the constituents approaches the light-cone -- i.e., $-\left(z^{(i)} - z^{(j)}\right)^2 \sim \left(z_\perp^{(i)} - z_\perp^{(j)}\right)^2 \to \mathcal{O}(1/Q^2)$. The distribution amplitude ϕ is the probability amplitude for finding the valence quarks sufficiently near the light-cone; by the uncertainty principle, this corresponds to a momentum space wavefunction smeared over all $k_\perp^2 \lesssim 1/z_\perp^2 \sim Q^2$ as in Eq. (1.7). Each (polynomial) eigensolution $\tilde{\phi}_n(x_i)$ [Eq. (1.9)] of the evolution equation is directly related to a term in the operator product expansion of the wave function evaluated near the light-cone. The eigenvalues γ_n are the corresponding anomalous dimensions.

Beyond leading order, both the hard-scattering amplitude and the potential in the evolution equation have expansions in $\alpha_s(Q^2)$:

$$T_H(x_i,y_i,Q) = \left(\frac{\alpha_s(Q^2)}{Q^2}\right)^2 \left\{T_o(x_i,y_i) + \alpha_s(Q^2)T_1(x_i,y_i) + \ldots\right\} \tag{1.11}$$

$$V(x_i,y_i,\alpha_s(Q^2)) = V_o(x_i,y_i) + \alpha_s(Q^2)V_1(x_i,y_i) + \ldots \quad .$$

These corrections can be systematically evaluated and the basic equations [Eqs. (1.5) and (1.8)] made exact to any order in $\alpha_s(Q^2)$.

An essential part of the derivation of these results is an analysis of the endpoint behavior of the x_i and y_i integrations in Eq. (1.5), and especially of the region $x_i \to 1$ or $y_i \to 1$. So long as $(1-x_i) >> m/Q$, we find that the distribution amplitude vanishes as $\phi(x_i,\tilde{Q}) \sim (1-x_i)^{\epsilon(\tilde{Q})}$ with $\epsilon(\tilde{Q}) > 1$ as $x_i \to 1$. This follows from a perturbative analysis of the $x_i \sim 1$ region coupled with the realization that $\epsilon(\tilde{Q}) \to 2$ as $Q \to \infty$, which is a necessary consequence of the evolution equation (1.8). Consequently ϕ and ϕ^* vanish sufficiently quickly that the x_i,y_i integrations are well behaved, at least for $(1-x_i) >> m/Q$. In particular, the evolution of the amplitude eliminates any potential logarithmic singularities in the region $1 >> (1-x_i) >> m/Q$.

The region $1-x_i \lesssim m/Q$ must be analyzed separately. Contributions from this region were first discussed by Drell and Yan, and West [14]. They related the Q^2 dependence of these contributions to the $x \sim 1$ behavior of the deep inelastic structure function νW_2. Taking $\nu W_2 \sim (1-x)^3$ as $x \to 1$, in accord (roughly) both with experiment and with naive theoretical expectations, the Drell-Yan-West connection implies a term in the form factor which falls as $1/Q^4$ -- i.e., just as in Eq. (1.10). However, a detailed examination reveals that this term is suppressed by at least two full powers of $\alpha_s(Q^2)$ relative to (1.10). Furthermore, in perturbation theory, gluonic corrections to the quark-photon vertex result in a Sudakov form factor which suppresses the endpoint contributions by an additional power $(m/Q)^6$. Thus the infinitesimal region $1-x_i \lesssim m/Q$ makes only a negligible contribution to the

form factor. It is also clear then that the Drell-Yan-West connection between deep inelastic scattering and hadronic form factors is invalid in QCD. It should be emphasized that, given that the Sudakov form factor S(Q) is a decreasing function of Q^2, the short distance domain where (1-x) >> m/Q gives the correct asymptotic QCD behavior for the baryon form factor up to corrections of relative order $\alpha_s^2(Q)S(Q)$ from the Drell-Yan-West region. In the case of meson form factors, $F_{\pi\gamma}(Q^2)$, $\gamma\gamma \to M\bar{M}$, etc., the endpoint region $(1-x) \lesssim m/Q$ is suppressed by a kinematic factor of m/Q allowing a direct proof of short distance dominance using operator product and renormalization group methods [1,2,6]. Further discussion of the exclusive-inclusive connection will be given in Sect. 4.

Following the above prescription, we can reduce the pion's electromagnetic form factor to the form:

$$F_\pi(Q^2) = \int_0^1 [dx][dy] \int \frac{d^2k_\perp d^2\ell_\perp}{(16\pi^3)^2} \psi^*(y_i,\ell_\perp) T(x_i,y_i,k_\perp,\ell_\perp,q_\perp) \psi(x_i,k_\perp)$$

$$= \int_0^1 [dx][dy]\ \phi^*(y_i,\tilde{Q}_y) \bar{T}_H(x_i,y_i,Q) \phi(x_i,\tilde{Q}_x) \qquad (1.12)$$

where T contains all two-particle irreducible amplitudes for $\gamma^* + q\bar{q} \to q\bar{q}$, and $\tilde{Q}_y = \min(y_i Q)$, $\tilde{Q}_x = \min(x_i Q)$. The leading contribution comes from one-gluon exchange

$$T_H(x_i,y_i,Q) = \frac{16\pi C_F \alpha_s(Q^2)}{Q^2} \left[\frac{e_1}{x_2 y_2} + \frac{e_2}{x_1 y_1}\right] \left[1 + \mathcal{O}\left(\alpha_s(Q^2), m/Q\right)\right] \qquad (1.13)$$

where e_1 and e_2 are the charges carried by particles 1 and 2 (in units of e). The properties of ϕ insure there is no singularity in (1.12) at y_i or $x_i \sim 0$. Consequently, in leading order, we can replace $\tilde{Q}_x$ and $\tilde{Q}_y$ by Q in (1.12) to obtain the QCD prediction for the pion form factor [1,8,9]

$$F_\pi(Q^2) = \frac{4\pi C_F \alpha_s(Q^2)}{Q^2} \left| \sum_{n=0,2,4,\ldots} a_n \left(\ell n \frac{Q^2}{\Lambda^2}\right)^{-\gamma_n} \right|^2 \left[1 + \mathcal{O}\left(\alpha_s(Q^2), m/Q\right)\right] . \qquad (1.14)$$

The $n=0$ term dominates as Q^2 becomes very large and we obtain [10]

$$F_\pi(Q^2) \to 16\pi\, \alpha_s(Q^2)\, \frac{f_\pi^2}{Q^2} \quad . \tag{1.15}$$

Thus, each hadronic scattering amplitude can be computed at large momentum transfer Q from a hard-scattering amplitude $T_H(x_i,Q,\theta_{c.m.})$ -- calculated by replacing each hadron by collinear on-shell valence quarks -- convoluted with the distribution amplitudes $\phi(x_i,\tilde{Q})$ for finding the constituents with light-cone momentum fractions x_i at transverse separations $\sim \mathcal{O}(1/\tilde{Q}^2)$, with $\tilde{Q} = (\min\, x_i)Q$. By definition, all loops containing collinear divergences are summed in the distribution amplitudes rather than in T_H. The gauge-invariant distribution amplitude $\phi(x_i,Q)$ plays the same role in exclusive amplitudes as the quark and gluon probability distribution functions $q(x,Q)$ and $g(x,Q)$ play in inclusive reactions [15]. In each case, the large Q^2 behavior of these functions can be analyzed from the operator product expansion or, equivalently, evolution equations

$$\partial F(x,Q^2)/\partial \log Q^2 = \int V\big(x,y,\alpha_s(Q)\big)F(y,Q^2)\,dy \tag{1.16}$$

with distinct kernels $V\big(x,y,\alpha_s(Q^2)\big)$ for each quantity. After renormalization, T_H and V can then be developed in a perturbative expansion in $\alpha_s(Q^2)$. All the results are covariant and gauge-invariant, although the analysis is most easily carried out in the light-cone gauge using light-cone perturbation theory (see Appendix A of Ref. [2]). The infrared singularity which occurs in the gauge-dependent anomalous dimension for colored fields in this gauge always cancels in physical matrix elements. A completely covariant analysis for $F_{\pi\gamma}(Q^2)$ and the connections with the Bethe-Salpeter wavefunction and the procedures required to extend the analyses to higher order in $\alpha_s(Q^2)$ are outlined in Ref. [2]. Alternatively, one could obtain the higher order connections by calculating the perturbative amplitude for the scattering of collinear, mass-less on-shell quarks to a given order, and then identify the contributions

not already included in the leading order results given here, in analogy to the methods used for inclusive processes.

The most important dynamical features of the hadronic amplitudes at large momentum transfer -- their power-law fall-off in Q^2, their angular dependence, and their helicity dependence -- are all determined by the Born contributions to $T_H(x_i,Q,\theta_{c.m.})$. We are thus lead to a large number of detailed, experimentally testable, predictions of QCD which critically reflect its elementary scaling and spin properties at short distances. In particular there are two sets of universal predictions of QCD which follow from the properties of $T_H(x,Q^2,\theta_{c.m.})$ to leading order in $1/Q$ and to <u>all orders</u> in $\alpha_s(Q^2)$ [1,2]:

(A) The dimensional counting rules for the power-law behavior of exclusive processes: $\mathcal{M} \sim Q^{4-n}$, where n is the minimum number of external elementary fields (leptons, quarks, transversely-polarized gluons or photons) participating in T_H.

(B) The QCD helicity selection rules: $\Delta h = 0$ (hadron helicity conservation).

In the case of electromagnetic or weak form factors, hadron helicity conservation leads to an even more restrictive rule: $|h| \leq 1/2$ (minimal helicity for each interacting hadron). These helicity rules are special features of a vector gluon gauge theory.

Thus form factors for processes in which the hadron's helicity is changed, or in which the initial or final hadron has helicity ≥ 1 are suppressed by powers of m/Q where m is an effective quark mass. Form factors for particles with opposite helicity dominate for q^2 timelike. The QCD selection rules imply power-law suppression of $F_2^N(Q^2)/F_1^N(Q^2)$, $\gamma^* p \to \Delta(h = 3/2)$, and $e^+e^- \to \bar{p}p$, $\rho_L\rho_T$, $\rho_T\rho_T$, $\Delta(h = 3/2) + \Delta(h = -3/2)$, etc. Further discussion is given in Sect. 2.

The techniques developed here can be readily extended to other hadronic systems, including large momentum transfer reactions involving nuclei, pure gluonic states, heavy quark bound states, etc. Applications to the elastic and inelastic weak and electromagnetic form factors of baryons are given in Ref. [4]. We have also used similar methods to analyze the endpoint $x \to 1$

behavior of meson and baryon structure and fragmentation functions in perturbative QCD, taking into account the correct kinematic limits on structure function evolution [1,6]. As we emphasize in Sect. 4, the Drell-Yan-West connection does not work in detail in QCD: for example, the perturbative diagrams which control the $x \to 1$ behavior of baryon structure functions (giving the nominal power $F_2(x) \sim (1-x)^3$) lead to contributions to baryon form factors which are suppressed by at least two powers of $\alpha_s(Q^2)$ and the Sudakov form factor. In the case of large angle exclusive hadron-hadron scattering processes, Sudakov form factors suppress the contribution of the Landshoff pinch singularities. [Discussions and references are given in Ref. 2.]

We can also apply the methods of this paper to the calculation of "high twist" subprocesses in inclusive reactions, such as C/Q^2 terms in the meson longitudinal structure function [16], power-law suppressed terms in the baryon structure function, and subprocesses involving more than the minimal number of interacting fields in high transverse momentum reactions [17] (see Sects. 4 and 6).

The testing of QCD in exclusive reactions is just beginning, but already there are a number of important phenomenological successes. The power-laws predicted by QCD for the pion, nucleon (and deuteron) form factors, and for large angle $pp \to pp$, $np \to np$, $\pi^{\pm}p \to \pi^{\pm}p$, $\gamma p \to \gamma p$, and $\gamma p \to \pi^+ n$ scattering are consistent with the data. A review is given in Ref. [2]. These scaling results give the best test so far for the essential scale invariance of $qq \to qq$ scattering and the q and g propagators. We emphasize that the specific integral powers predicted by perturbative QCD reflect both the scale-invariance of the basic interactions and the fact that the minimal color singlet wavefunctions of hadrons contain either 3 quarks or quark plus antiquark (or 2 or 3 gluons). The dynamics and symmetries of QCD are thus directly tested. The fact that logarithmic modifications are not yet apparent in the data -- particularly in $s^{10}d\sigma/dt(pp \to pp)$, which should roughly scale at fixed angle as $\alpha_s^{10}(s)$, gives evidence that $\alpha_s(Q^2)$ is slowly varying -- i.e., that the QCD

scale-constant Λ is relatively small: $\Lambda_{eff} \lesssim 100$ to 300 MeV. [The larger value is only possible if mass corrections are important.]

A more qualitative success of QCD is the fact that the pion form factor, computed with the asymptotic wavefunction normalized to the pion decay constant, is within a factor of ~2 of the observed space-like data. The definitive check of the predictions for $F_\pi(Q^2)$ will require an evaluation of the order $\alpha_s(Q^2)$ correction, as well as further constraints on the pion distribution amplitude $\phi(x,Q)$. As we shall show in Sect. 5, measurements of the scaling properties and angular dependence of the two-photon processes $d\sigma/dt(\gamma\gamma \to M\bar{M})$, with $M = \pi^{\pm,0}$, $\rho_{L,T}^{\pm,0}$ and their ratio to the corresponding $e^+e^- \to M^+M^-$ cross sections can provide extraordinary checks on QCD and important constraints on the form of the distribution amplitudes at non-asymptotic momenta. These two-photon processes are the simplest non-trivial hadronic scattering amplitudes computable in perturbative QCD. Pinch contributions are power-law suppressed in this case. We also emphasize the importance of experimentally checking the ratio of π^+ to K^+ to ρ_L^+ form factors which are predicted to asymptotically approach the ratios $f_\pi^2 : f_K^2 : 2f_\rho^2 \sim 1 : 1.5 : 2.5$. The fact that the pion form factor has the same sign as its value at $Q^2 = 0$ (i.e., no zeroes) is a non-trivial check of QCD; for scalar gluons, the meson form factor would change sign as Q^2 increases. Another qualitative success of QCD is its apparent explanation of the surprisingly large normalization of the $pp \to pp$ and $\pi p \to \pi p$ scattering amplitudes and the magnitude of large momentum transfer nuclear form factors. It remains an open question whether the large spin polarization observed in large angle $pp \to pp$ scattering at Argonne can be explained in terms of perturbative QCD mechanisms.

2. Constraints on Hadronic Wavefunctions

The quark distribution amplitudes $\phi(x_i,Q) \sim \int^Q d^2k_\perp \psi(x_i,k_{\perp i})$ which control exclusive reactions at large momentum transfer, and the quark probability distributions $q(x_i,Q) \sim \int^Q d^2k_\perp |\psi(x_i,k_{\perp i})|^2$ (summed over all Fock states), which control inclusive reactions at large momentum transfer, are each determined by the hadronic Fock state wavefunctions $\psi(x_i,k_{\perp i})$. In principle the $\psi(x_i,k_{\perp i})$ describe all hadronic matrix elements. A central goal of hadronic physics will be to utilize these wavefunctions to unify short and long distance physics, and make contact with hadronic spectroscopy, low momentum transfer reactions, and the whole range of non-perturbative physics.

Although the complete specification of hadronic wavefunctions clearly will require a solution of the non-perturbative bound state problem in QCD, there is a large number of properties of the wavefunctions which can be derived from the theory and experimental phenomena. In this section we will discuss the following constraints [3]:

(a) The predictions of perturbative QCD for the large transverse momentum tail of the Fock state infinite momentum wavefunction $\psi(k_{\perp i},x_i)$. These results, which also follow from the operator product expansion near the light-cone [13], lead to evolution equations [1,2] for the process-independent distribution amplitudes $\phi(x_i,Q)$ which control large transverse momentum exclusive reactions such as form factors, and for the distribution functions $G_{q/H}(x_i,Q)$ and $G_{g/H}(x_i,Q)$ which control large transverse momentum inclusive reactions.

(b) Exact boundary conditions for the valence Fock state meson wavefunctions from the meson decay amplitudes. In particular we shall show how the $\pi^o \to \gamma\gamma$ decay amplitude for massless quarks specifies the pion wavefunction at zero $k_\perp$. This is a new type of low energy theorem for the pion wavefunction which is consistent with chiral symmetry and the triangle anomaly for the axial vector current [18]. This large-distance result, together with the constraint on the valence wavefunction at short distance from the $\pi \to \mu\nu$ leptonic decay amplitude, leads to a number of new results for the parameterization of the

pion wavefunction. In particular, we show that the probability of finding the valence $|q\bar{q}\rangle$ state in the total pion wavefunction is ~0.2 to 0.25, for a broad range of confining potentials.

(c) As noted above the wavefunction for the Fock states of the hadrons on the light-cone (or at infinite momentum frame) $\psi^{(n)}_{S_z}(k_{\perp i}, x_i, s_i)$ completely specify the quark and gluon particle content of the hadrons. The coherent aspects of the wavefunction are required for constructing the distribution amplitudes which are not only necessary for exclusive processes, but also for the multi-particle, high twist subprocesses which enter inclusive reactions and control transverse momentum smearing effects. We show that the evolution equations which specify the large Q^2 behavior of the distribution amplitudes and of incoherent distribution functions G are correctly applied for $Q^2 \gtrsim \langle \mathscr{E} \rangle$, where $\langle \mathscr{E} \rangle$ is the mean value of the off-shell (light-cone/infinite momentum frame) energy in the Fock state wavefunction

$$\mathscr{E} \equiv \sum_i \mathscr{E}_i \equiv \sum_{i=1}^{n} \left(\frac{k_\perp^2 + m^2}{x} \right)_i \quad . \tag{2.1}$$

To first approximation, $\langle \mathscr{E} \rangle$ is the "starting point" Q_0^2 for evolution due to perturbative effects in QCD.

Let us now discuss the constraints on meson wavefunctions imposed by their decay constants. The leptonic decays of the mesons give an important constraint on the valence $|q\bar{q}\rangle$ wavefunction at the origin. As shown in Ref. [1,2]

$$\lim_{Q \to \infty} \phi_M(x_i, Q) = a_0 x_1 x_2 = \begin{cases} \frac{3}{\sqrt{n_c}} f_\pi x_1 x_2 & \text{for } \pi \\ \\ \frac{3\sqrt{2}}{\sqrt{n_c}} f_\rho x_1 x_2 & \text{for } \rho_L \end{cases} \tag{2.2}$$

where $f_\pi \cong 93$ MeV is the pion decay constant for $\pi^+ \to \mu^+ \nu$ and $f_\rho \cong 107$ MeV is the leptonic decay constant from $\rho^o \to e^+ e^-$. The analogous result holds for all zero helicity mesons. Because the $Q^2 \to \infty$ distribution amplitude has zero

anomalous dimension, this constraint is independent of gluon radiative correction and can be applied directly to the non-perturbative wavefunction:

$$a_0 = 6\int [dx][d^2k_\perp]\, \psi_M^{\text{non-pert}}(k_\perp, x) \quad . \tag{2.3}$$

On the other hand we can also obtain an exact low energy constraint on $\psi(k_\perp = 0, x)$ for the pion in the chiral limit $m_q \to 0$. The $\gamma^* \pi^0 \to \gamma$ vertex defines the $\pi^0 - \gamma$ transition form factor $F_{\pi\gamma}(Q^2)$ $(q^2 = -Q^2)$,

$$\Gamma_\mu = -ie^2 F_{\pi\gamma}(Q^2)\, \varepsilon_{\mu\nu\rho\sigma} P_\pi^\nu \epsilon^\rho q^\sigma \quad , \tag{2.4a}$$

where

$$F_{\pi\gamma}(0) = \frac{1}{4\pi^2} n_c \left(e_u^2 - e_d^2\right) \frac{1}{f_\pi} \quad . \tag{2.4b}$$

This result, derived by the Schwinger, Adler, Bell and Jackiw [18], gives for $n_c = 3$ the $\pi^0 \to \gamma\gamma$ decay rate, $\Gamma_{\pi^0 \to \gamma\gamma} = \frac{\pi\alpha^2}{2} m_\pi^3 F_{\pi\gamma}^2(0) = 7.63$ eV compared to $\Gamma_{\text{expt}} = (7.95 \pm 0.55)$ eV.

If $m_q \to 0$, then the valence $|q\bar{q}\rangle$ contribution to $F_{\pi\gamma}(Q^2)$ is [2]

$$F_{\pi\gamma}(Q^2) = 2\sqrt{n_c}\left(e_u^2 - e_d^2\right)\left\{\int_0^1 dx_1 \int_0^{x_1^2 Q^2} \frac{dk_\perp^2}{16\pi^2} \frac{\psi(k_\perp, x_1)}{Q^2 x_1} + (x_1 \leftrightarrow x_2)\right\} . \tag{2.5}$$

In fact, as shown in Ref. [19], gauge-invariance requires that the valence $|q\bar{q}\rangle$ state should give exactly 1/2 of the total decay amplitude for $q^2 \to 0$. Thus from Eqs. (2.4b) and (2.5), we find

$$\psi\left(k_\perp = 0, x_1\right) = \frac{\sqrt{n_c}}{f_\pi} \quad . \tag{2.6}$$

Therefore the pion wavefunction is constrained both at large and small distances.

In order to implement these constraints it is convenient to construct a simple model of the hadronic wavefunction. By using the connection (2.19) below for the two particle state from the harmonic oscillator model [20] we can get the wavefunction in the infinite momentum frame

$$\psi^{(2)}(k_\perp, x_i, s_i) = A \exp\left[-R^2\left(\frac{\vec{k}_\perp^2 + m_q^2}{x_1} + \frac{\vec{k}_\perp^2 + m_q^2}{x_2}\right)\right] \quad . \tag{2.7}$$

Perhaps the simplest generalization for the n-particle Fock state wavefunctions in the non-perturbative domain is the Gaussian form:

$$\psi^{(n)}_{S_z}(k_{\perp i}, x_i, s_i) = A_n \exp\left[-R_n^2\right]$$
$$= A_n \exp\left[-R_n^2 \sum_{i=1}^{n}\left(\frac{\vec{k}_\perp^2 + m^2}{x}\right)_i\right] \quad . \tag{2.8}$$

The parameterization is taken to be independent of spin. The full wavefunction is the $\psi^{(n)}_{S_z}(k_{\perp i}, x_i, s_i)$ multiplied by the free spinor $u(k_i, s_i)/\sqrt{k_i^+}$ or $v(k_i, s_i)/\sqrt{k_i^+}$. The Gaussian model corresponds to a harmonic oscillator-confining potential $V \propto \vec{r}^2$ in the CM frame. This ansatz for the wavefunction has the additional analytic simplicity of (a) factorizing in the kinematics of each constituent and (b) satisfying a "cluster" property when the constituents are grouped into any rearrangement of subcomposites A,B,...

If we adopt the Gaussian form for the meson wavefunction Eq. (2.7) then constrains (2.3) and (2.6) imply $\left(m_q^2 R^2 << 1,\ n_c = 3\right)$

$$R = \frac{1}{4\pi f_\pi} \simeq 0.17 \text{ fm} \quad ,$$

and

$$A = \frac{\sqrt{3}}{f_\pi} e^{2m_q^2 R^2} \quad . \tag{2.9}$$

The probability of finding the valence $q\bar{q}$ state in the π ion is thus

$$P(q\bar{q}) = \int [dx][d^2k_\perp]\ |\psi(x_\perp, x_i)|^2 = \frac{1}{4} \quad . \tag{2.10}$$

Alternatively, if we use a power-law form

$$\psi(k_\perp, x_i) = \frac{A_\alpha}{\left(\frac{k_\perp^2 + m_q^2}{x(1-x)} + \mu^2\right)^\alpha} \tag{2.11}$$

we find ($m_q^2 \ll u^2$)

$$P(q\bar{q}) = \frac{1}{2}\,\frac{\alpha-1}{2\alpha-1} \quad , \tag{2.12}$$

which again leads to 1/4 for large α. For the linear potential case, where $\alpha = 3$, we have $P(q\bar{q}) = 1/5$.

Let us consider the implications of these results for exclusive large momentum transfer processes. As discussed in Sect. 1, we require the behavior of the distribution amplitude $\phi(x_i,s_i,Q^2)$ defined in Eq. (1.7), which is the probability for finding valence quarks at relative transverse separation $b_\perp \sim O(1/Q)$. The large Q^2 dependence of ϕ (i.e., the large $k_\perp$ tail of ψ) is in fact completely determined by the operator product expansion near the light-cone, and in QCD can be calculated from the perturbative expansion in the irreducible kernel for the quark constituents. To order $\alpha_s(Q^2)$ one only requires single gluon exchange, and we find, using the evolution equation [1,2]

$$\phi(x_i,Q^2) = \phi(x_i,Q_0^2) + \frac{C_F}{\beta}\int_{Q_0^2}^{Q^2}\frac{d\ell_\perp^2}{\ell_\perp^2}\int[dy]\;\alpha_s\left(\frac{\ell_\perp^2}{y_i(1-y_i)}\right)$$

$$\times\left[V(x_i,y_i) - \delta(x-y)\right]\phi(y_i,\ell_\perp^2) \quad , \tag{2.13}$$

where

$$V(x,y) = 2\left\{x_1y_2\theta(y_1-x_1)\left(\delta_{h_1\bar{h}_2} + \frac{\Delta}{y_1-x_1}\right) + (1\leftrightarrow 2)\right\}$$

$$= V(y,x) \quad . \tag{2.14}$$

This result is derived in the region $\ell_\perp^2/y_1(1-y_1)$ is large compared to the off-shell energy $\langle\mathscr{E}\rangle$ in the wavefunction. Thus the natural starting point for the evolution of the distribution amplitude is $[Q_0^2/x_1(1-x_1)] \sim \langle\mathscr{E}\rangle$, i.e., to the first approximation we can identify

$$\phi(x_i,Q^2) = \phi^{\text{non-pert}}(x_i) + \frac{C_F}{\beta}\int_{x_1(1-x_1)\langle\mathscr{E}\rangle}^{Q^2}\frac{d\ell_\perp^2}{\ell_\perp^2}\int[dy]\;\alpha_s\left(\frac{\ell_\perp^2}{y_1(1-y_1)}\right)$$

$$\times\left[V(x,y) - \delta(x-y)\right]\phi(y_1,\ell_\perp^2) \quad , \tag{2.15}$$

where

$$\phi^{\text{non-pert}}(x_i) = \int\left[d^2k_\perp\right]\psi^{\text{non-pert}}\left(\vec{k}_\perp^2, x_i\right) \quad . \tag{2.16}$$

Assuming the wavefunction given by Eqs. (2.7) and (2.9), the shape and the normalization of $\phi^{\text{non-pert}}(x_i)$ depends only upon the quark mass. The application of perturbative QCD for $\left[\ell_\perp^2/y_1(1-y_1)\right] \gtrsim \langle\mathcal{E}\rangle$ is reasonable here, since $\langle\mathcal{E}\rangle \sim 0.7\ \text{GeV}^2$ for this wavefunction is much larger than QCD Λ^2_{eff}.

An (approximate) connection between the equal-time wavefunction in the center of mass frame and the infinite momentum frame wavefunction can be established by equating the energy propagator $M^2 - \mathcal{E} = M^2 - \left(\sum_{i=1}^{n} k_i^\mu\right)^2$ in the two frames:

$$M^2 - \mathcal{E} = \begin{cases} M^2 - \left(\sum_{i=1}^{n} q^o_{(i)}\right)^2 & \sum_{i=1}^{n} \vec{q}_i = 0 \quad [\text{CM}] \\ M^2 - \sum_{i=1}^{n}\left(\dfrac{\vec{k}_\perp^2 + m^2}{x}\right) & \sum_i \vec{k}_{\perp i} = 0 \\ & \sum_i x_i = 1 \quad [\text{IMF}] \end{cases} \quad . \tag{2.17}$$

Thus the rest frame wavefunction $\psi_{CM}\left(\vec{q}_{(i)}\right)$ which controls binding and hadronic spectroscopy implies a form for the IMF wavefunction $\psi_{IMF}\left(x_i, k_{\perp i}\right)$ if we kinematically identify

$$x_i \equiv \frac{k_i^+}{P^+} \leftrightarrow \frac{\left(q^0 + q^3\right)_i}{\sum_j^n q_j^o} \quad , \tag{2.18}$$

and

$$\vec{k}_{\perp i} \leftrightarrow \vec{q}_{\perp i} \quad .$$

For a two particle state, there is thus a possible connection;

$$\psi_{IMF}\left(\frac{k_\perp^2 + m^2}{1 - x^2} - m^2\right) \leftrightarrow \psi_{CM}\left(\vec{q}^2\right) \quad , \quad \left(x = x_1 - x_2\right) \quad . \tag{2.19}$$

An equivalent result was also obtained recently by Karmonov [21] using a different method.

Let us, for illustration and simplicity assume the n-particle Fock state wavefunction $\psi^{(n)}$ is a symmetric function of the relativistic kinetic energy $\mathscr{E}_i = \left[(\vec{k}_\perp^2 + m^2)/x\right]_i$. Independent of the form of ψ, it is easy to show

$$G_{a/\Sigma}^{\text{non-pert}}(x_a) \underset{x_a \to 1}{\longrightarrow} (1-x_a)^{2n_s - 1} F\left(\mathscr{E}^i_{\min}\right) \quad , \tag{2.20}$$

where $n_s = \min(n_H - n_a)$ is the minimum number of spectator constituents in the hadron H after removing the particle (or subcomposite) a, and $\mathscr{E}^i_{\min} = m_i^2/x_i$ is the minimum value of $\mathscr{E}_i$. This result which follows from the definition (1.3) by changing variables from $d^2k_{\perp i}$ to $d^2k_{\perp i}/x_i$ is independent of the form of $\psi(\mathscr{E}_i)$ as long as it is square-integrable under $[d^2k_\perp]$. Examples of this result for $G_{q/M}$ and $G_{q/B}$ have recently been given by de Rujula and Martin [22]. Notice that if we can neglect the quark masses (i.e., for $(1-x_a) >> m^2/\langle k_\perp^2\rangle$) we obtain the spectator rule proposed in Ref. [23]

$$G_{a/H}^{\text{non-pert}}(x_a) = C_{a/H}(1-x_a)^{2n_s - 1} \quad ,$$
$$\left(x_a \sim 1 \quad , \quad (1-x_a) >> \frac{m^2}{\langle k_\perp^2\rangle}\right) \quad . \tag{2.21}$$

In fact if we neglect $m^2/\langle k_\perp^2\rangle$ the non-perturbative contribution can dominate the perturbative prediction in the $x \sim 1$ domain! For example, the perturbative power-law behavior is [24]

$$\Delta G_{q/M}^{\text{pert}} \underset{x \to 1}{\sim} \alpha_s^2 (1-x)^2 \quad , \tag{2.22}$$

and [25]

$$\Delta G_{q/B}^{\text{pert}} \underset{x \to 1}{\sim} \alpha_s^4 \begin{cases} (1-x)^3 \text{ parallel q and B helicity} \\ (1-x)^5 \text{ anti-parallel q and B helicity} \end{cases} . \tag{2.23}$$

Since flavor and spin are correlated in the baryon wavefunction, perturbative QCD predicts $\Delta G_{u/P} \neq 2\Delta G_{d/P}$. In fact if we assume the baryon wavefunction satisfies SU(6) symmetry (which is a rigorous result for $\phi_B(x_i, Q)$, $Q \to \infty$), we have $\Delta G_{u/P} = 5\Delta G_{d/P}$ for $x \to 1$ [25]. The question of whether the non-

perturbative or perturbative contribution dominates the structure functions at $x \to 1$ can thus be studied using spin and flavor correlations.

3. Form Factors and Hadronic Wavefunctions

Figure 3 illustrates the QCD predictions for Q^2F_π given three different initial wavefunction at $Q_0^2 = 2$ GeV^2 [26]:

$$\begin{aligned} &(a)\quad \phi(x_i,Q_0) \propto x_1x_2 \\ &(b)\quad \phi(x_i,Q_0) \propto \delta(x_i - 1/2) \\ &(c)\quad \phi(x_i,Q_0) \propto (x_1x_2)^{1/2} \end{aligned} \tag{3.1}$$

with representative values of the QCD scale parameter Λ^2. In each case the normalization is uniquely determined by (2.2); all curves ultimately converge to the asymptotic limit (1.15). For Fig. 3, we have multiplied (1.14) by $(1+m_\rho^2/Q^2)^{-1}$ to allow a smooth connection with the low Q^2 behavior suggested by vector dominance models.

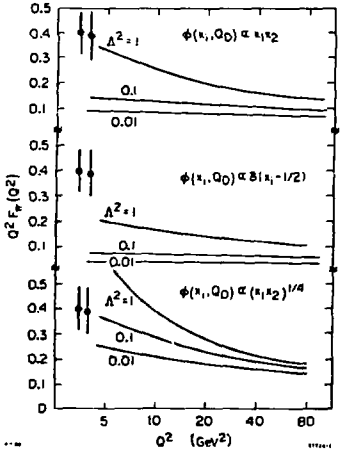

Fig. 3. QCD predictions for the pion form factor assuming various distribution amplitudes $\phi(x_i,Q_0)$ at $Q_0^2 = 2$ GeV^2 and various values of the QCD scale parameter Λ^2. The data are from the analysis of electroproduction $e^-p \to e^- + \pi^+ + n$; C. Bebek et al., Ref. [26].

The behavior exhibited in Fig. 3 can be radically modified if $\phi(x_1,Q_0)$ has nodes or other complex structure in x_1. However such behavior is unlikely for ground state mesons such as the pion. For these, one intuitively expects a smooth, positive-definite distribution amplitude, peaked about $x_1,x_2 \sim 1/2$. Given these constraints, the normalization of $F_\pi(Q^2)$ is largely determined by the breadth of the distribution -- broad distributions (Fig. 3c) result in a large form factor, narrow distributions (Fig. 3b) in a small one. The magnitude of the form factor also depends to some extent upon the scale parameter Λ^2 through the factor $\alpha_s(Q^2)$ in (1.14).

Notice that we can completely remove dependence upon the distribution amplitude by comparing $F_{\pi\gamma}$ to F_π. In fact a measurement of each provides a direct determination of $\alpha_s(Q^2)$:

$$\alpha_s(Q^2) = \frac{n_c\left(e_u^2 - e_d^2\right)^2}{\pi C_F} \frac{F_\pi(Q^2)}{Q^2\left|F_{\pi\gamma}(Q^2)\right|^2} + O\left(\alpha_s^2(Q^2)\right)$$

$$= \frac{1}{4\pi} \frac{F_\pi(Q^2)}{Q^2\left|F_{\pi\gamma}(Q^2)\right|^2} + O\left(\alpha_s^2(Q^2)\right) \quad . \tag{3.2}$$

The electromagnetic form factors of K^+-meson and longtiudinally polarized ρ^+-mesons follow from the same analysis but with f_π replaced in the sum rule by f_K and $\sqrt{2}\, f_\rho$ respectively. If the quark distribution amplitudes for these different mesons are similar in shape, the ratios of π to K to ρ_L form factors should be approximately $f_\pi^2 : f_K^2 : 2f_\rho^2 \sim 1 : 1.5 : 2.5$ for Q^2 large (becoming exact as $Q^2 \to \infty$).

An important constraint on the nature of the distribution amplitude for K-mesons can be obtained from the K_L-K_S transition form factor which is measurable at large timelike Q^2 in the reaction $e^+e^- \to K_L K_S$. The K^o wave-function

$$\psi_{K^o} = \frac{\delta_{ba}}{\sqrt{n_c}} \frac{1}{\sqrt{2}} \left\{ d_\uparrow \bar{s}_\downarrow - d_\downarrow \bar{s}_\uparrow \right\} \frac{\psi_{K^o}\left(x_i,k_{i\perp}\right)}{\sqrt{x_s x_d}} \tag{3.3}$$

where, because of the large m_s/m_d ratio, Ψ_{K^0} need not be symmetric in $x_s \leftrightarrow x_d$. The transition form factor $F_{K_S \to K_L}(Q^2)$ at large Q^2 can then be written in the form of Eq. (1.12) with

$$T_H(x_i,y_i,Q) = \frac{16\pi\alpha_s(Q^2)C_F}{Q^2}\left[\frac{e_s}{x_d y_d} + \frac{e_d}{x_s y_s}\right] , \qquad (3.4)$$

and thus

$$F_{K_S \to K_L}(Q^2) = \left(\frac{1}{3}\right)\frac{8\pi\alpha_s(Q^2)C_F}{Q^2}\left[\sum_{n(\text{even})}\sum_{m(\text{odd})} a_n^* a_m \left(\ell n \frac{Q^2}{\Lambda^2}\right)^{-\gamma_n-\gamma_m} + \text{h.c.}\right]$$

$$\times \left[1 + O\left(\alpha_s(Q^2), m/Q\right)\right] . \qquad (3.5)$$

Thus the form factor requires the odd (asymmetric under $x = x_d - x_s \to -x$) Gegenbauer components of the K^0 distribution amplitude. Asymptotically, the transition form factor vanishes with an extra anomalous dimensions:

$$\frac{F_{K_S \to K_L}(Q^2)}{F_{K^+}(Q^2)} \underset{Q^2\to\infty}{=} \left(\frac{4}{3}\right) \text{Re}\left(\frac{a_1}{a_0}\right)\left(\ell n \frac{Q^2}{\Lambda^2}\right)^{-\gamma_1} \qquad (3.6)$$

where $\gamma_1 = (8/3)(C_F/\beta)$ ($\cong 0.4$ for $n_f = 3$). If this ratio of form factors is indeed appreciable [i.e., of order 1], then the odd, asymmetric components play a major role in the structure of the kaon wavefunction. This would also imply a strong violation of the relation $F_{\pi^+}(Q^2)/F_{K^+}(Q^2) \cong f_\pi^2/f_K^2$ at sub-asymptotic Q^2. All of these results can, of course, be extended to mesons containing heavy quarks.

Since quark helicity is conserved at each vertex in T_H, it is diagonal in hadronic helicity up to corrections of order m/Q. Further, to leading order in $1/Q^2$ only terms with $\sum_i s_i = S_z$ contribute in $\phi(x_i,Q)$. Consequently there are two selection rules restricting the helicities of initial (h_i) and final (h_f) hadrons [1,2,27]:

$$\begin{aligned} &\text{(a)} \quad \Delta h = h_f - h_i = 0 \qquad (\text{for timelike photon: } h_1 = -h_2) \\ &\text{(b)} \quad |h| = |h_{i,f}| \le 1/2 \quad . \end{aligned} \qquad (3.7)$$

The second rule is easily derived from the first in the Breit frame. There the net change in the hadron's angular momentum along the direction of motion is $\Delta J_z = -h_f - h_i = -2h$, because the helicity is unchanged while the momentum is reversed. As the photon has spin 1, only $|h| \leq 1/2$ is permitted, up to corrections of $O(m/Q)$.

Applying these selection rules to e^+e^- collisions beyond the resonance region, for example, we find that the final states $\pi\rho$, $\rho_L\rho_\perp$, $\rho_\perp\rho_\perp$ are suppressed by $\sim m^2/Q^2$ (in the cross section) relative to $\pi\pi$, KK and $\rho_L\rho_L$ final states.

The selection rules are direct consequences of the vector nature of the gluon. In contrast, $e^+e^- \to \rho_\perp\rho_\perp$ is <u>not</u> suppressed in a theory with scalar gluons. Furthermore while each of the 'allowed' form factors is positive at large Q^2 in QCD, they are negative in scalar gluon theories, and then must vanish at some finite Q^2 (since $F(0) = 1$). Scalar theories are probably already ruled out by existing data.

In the case of baryons, the evolution equation to leading order in $\alpha_s(Q^2)$ has a general solution of the form

$$\phi(x_i,Q) = x_1x_2x_3 \sum_{n=0}^{\infty} a_n \tilde{\phi}_n(x_i) \left(\ell n \frac{Q^2}{\Lambda^2}\right)^{-\gamma_n^N} + Cx_1x_2x_3 \begin{cases} \left(\ell n \frac{Q^2}{\Lambda^2}\right)^{-2/3\beta} & |h| = 1/2 \\ \left(\ell n \frac{Q^2}{\Lambda^2}\right)^{-2/\beta} & |h| = 3/2 \end{cases} \tag{3.8}$$

where the leading $\tilde{\phi}_n$, γ_n^N are given in Ref. [2], and h is the total quark helicity (= hadron's helicity since $L_z = 0$). However in practice it is generally more efficient to integrate the evolution equation numberically rather than expanding ϕ as in (3.8).

Convoluting the hard-scattering amplitude T_H (see Fig. 2) with $\phi(x_i,Q)$ then gives the QCD prediction [1,2]

$$G_M(Q^2) = \frac{32\pi^2}{9}\,\frac{\alpha_s^2(Q^2)}{Q^4}\sum_{n,m} b_{nm}\left(\ln\frac{Q^2}{\Lambda^2}\right)^{-\gamma_n^N-\gamma_m^N}\left[1+O\left(\alpha_s(Q^2),\frac{m^2}{Q^2}\right)\right]$$

$$+\frac{32\pi^2}{9}\,C^2\,\frac{\alpha_s^2(Q^2)}{Q^4}\left(\ln\frac{Q^2}{\Lambda^2}\right)^{-4/3\beta}(-e_{-\|}) \qquad (3.9)$$

where $e_\|$ ($e_{-\|}$) is the mean total charge of quarks with helicity parallel (anti-parallel) to the nucleon's helicity (in the fully symmetric flavor-helicity wavefunction). For protons and neutrons we have

$$e_\|^p = 1 \quad ; \quad e_{-\|}^p = 0 \quad ; \quad e_\|^n = -e_{-\|}^n = -1/3 \quad . \qquad (3.10)$$

The constants b_{nm}, C are generally unknown for baryons; however, by isospin symmetry, they are equal for protons and neutrons, and thus QCD predicts the ratios of form factors as $Q^2 \to \infty$.

Figure 4 illustrates the predictions for $Q^4G_M^p(Q^2)$ assuming a wavefunction $\phi(x_1,Q_0) \propto \delta(x_1 - 1/3)\delta(x_2 - 1/3)$ at $Q_0^2 = 2$ GeV^2 (the absolute normalization is undetermined) and various values of the QCD scale parameter [28]. Again we include an extra factor $(1+.71/Q^2)^{-2}$ in (3.9) to allow a smooth connection with data at low Q^2. Similar curves are obtained for any reasonably smooth

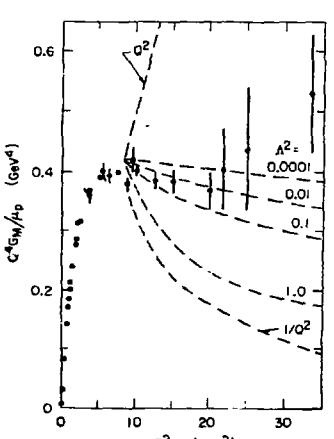

Fig. 4. (a) Prediction for $Q^4G_M^p(Q^2)$ for various QCD scale parameters Λ^2 (in GeV^2). The data are from Ref. [28]. The initial wavefunction is taken as $\phi(x_i\lambda) \propto \delta(x_1 - 1/3)\delta(x_2 - 1/3)$ at $\lambda^2 = 2$ GeV^2. The factor $(1+m_p^2/Q^2)^{-2}$ is included in the prediction as a representation of mass effects, and the overall normalization is unknown.

distribution amplitude $\phi(x_i,Q_0)$. Only the ratio $G_M^p(Q^2)/G_M^n(Q^2)$ is particularly sensitive to the shape of the distribution amplitude. For illustration, this ratio is plotted versus η in Fig. 5 where $\phi(x_i,Q) = (x_1x_2x_3)^\eta$ is assumed for a given Q^2. For each choice of η, the ratio decreases to zero with increasing Q^2 as $\left(\ell n\, Q^2/\Lambda^2\right)^{\gamma_0 - \gamma_3} = \left(\ell n\, Q^2/\Lambda^2\right)^{-32/9\beta}$. The ratio $G_M^p/G_M^n = -1$ at Q_0^2 for the δ-function distribution amplitude used in Fig 4. For comparison, note that in a theory with scalar or pseudo-scalar gluons, diagrams in which the struck quark has anti-parallel helicity vanish. Thus scalar QCD predicts a ratio $G_M^p/G_M^n \to e_\parallel^p/e_\parallel^n = -1/3$ independent of the distribution amplitude (assuming only symmetry under exchange $x_1 \leftrightarrow x_3$).

As for mesons, form factors for processes in which the baryon's helicity is changed ($\Delta h \neq 0$), or in which the initial or final baryon has $|h| > 1$, are suppressed by factors of m/Q, where m is an effective quark mass. Thus the helicity-flip nucleon form factor is predicted to fall roughly as $F_2 \sim mM/Q^6$. The reaction $e^+e^- \to \Delta^+\Delta^-$ is dominated by baryons with $|h_\Delta| = 1/2$; the cross section for production of $|h_\Delta| = 3/2$ pairs or deltas with $|h_\Delta| = 3/2$ and 1/2 is suppressed. Again most of these predictions test the spin of the gluon. For example, transitions $ep \to e\Delta$ ($|h_\Delta| = 3/2$) are not suppressed in scalar QCD.

An important feature of the perturbative QCD predictions -- again true to *all* orders in $\alpha_s(Q^2)$ -- is that all of the helicity-conserving electroweak form factors [4] involving nucleons can be expressed as linear combinations

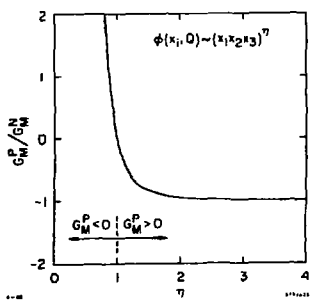

Fig. 5. The ratio of proton to neutron magnetic form factors for various distribution amplitudes.

of just two basic form factors -- $G_{\uparrow\uparrow}(Q^2)$ and $G_{\uparrow\downarrow}(Q^2)$ -- corresponding to amplitudes in which the current interacts with a valence quark with helicity parallel or anti-parallel to the helicity of the nucleons, respectively. The coefficients are determined by the corresponding $SU(2)_L \times U(1)$ quark charges. Thus the nucleon magnetic form factors $G_M^n(Q^2)$ and $G_M^p(Q^2)$ are sufficient to predict the weak nucleon form factors. The assumption of the standard helicity-flavor symmetry for the baryon wavefunctions at short distances then leads to the specification of all the leading electroweak octet and decouplet form factors. The spatial wavefunctions can be assumed to be symmetrical with respect to the quarks having the same helicity, a feature which is preserved under perturbative QCD evolution. At $Q^2 \to \infty$, the spatial wavefunction becomes totally symmetric, $\phi_B(x_i,Q) \to x_1 x_2 x_3 \left(\log Q^2/\Lambda^2\right)^{-\gamma_B}$, and thus the helicity-flavor structure of the baryon states satisfies exact SU(6) symmetry. The detailed results are given in Ref. [4].

4. Perturbative QCD Predictions for the $x \sim 1$ Behavior of Structure Functions -- QCD Evolution and High Twist Contributions

As we have emphasized in Sect. 2, one of the most important areas of study of perturbative quantum chromodynamics is the behavior of the hadronic wavefunctions at short distances or at far off-shell kinematics. This behavior can be tested not only in exclusive reactions such as form factors at large momentum transfer but also in deep inelastic scattering reactions at the edge of phase space. In this section we will review the QCD predictions for the behavior of the hadronic structure functions $F_1(x,Q)$ in the endpoint $x_{B_j} \sim 1$ region [6,29]. The endpoint region is particularly interesting because one must understand in detail (a) the contributions of exclusive channels, (b) the effect of high twist terms (power-law scale-breaking contributions) which can become dominant at large x, and (c) the essential role of the available energy W in controlling the logarithmic evolution of the structure functions. Note that as $x \sim 1$, essentially all of the hadron's momentum must be carried

by one quark (or gluon), and thus each propagator which transfers this momentum becomes far-off shell: $k^2 \sim -\left(\vec{k}_\perp^2 + \mathcal{M}^2\right)/(1-x) \to -\infty$ [see Fig. 6]. Accordingly, if the spectator mass $\mathcal{M}$ is finite the leading power-law behavior in (1-x) is determined by the minimum number of gluon exchanges required to stop the hadronic spectators, and only the valence Fock states, $|qqq\rangle$ for baryons, and $|q\bar{q}\rangle$ for mesons, contribute to the leading power behavior. If one simply computes the connected tree graphs, as in Fig. 7, then the perturbative (1-x) power-law behavior is given by Eqs. (2.22) and (2.23) of Sect. 2.

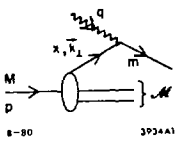

Fig. 6. Kinematics for inelastic structure functions.

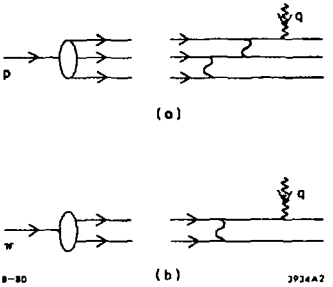

Fig. 7. Perturbative QCD tree diagrams for computing the $x \sim 1$ power behavior of baryon and meson structure functions.

Let us now consider how these results for the power-law behavior emerge within the complete perturbative structure of QCD. Including corrections from gluon radiation, vertex and self-energy corrections, and continued iteration of the gluon-exchange kernel, one finds for the nucleon's quark distribution [29].

$$G_{q/p}(x,Q) \underset{x\to 1}{=} (1-x)^3 \alpha_s^4(k_x^2) \left| \sum_{j=0}^{\infty} b_j \left(\log \frac{k_x^2}{\Lambda^2} \right)^{-\gamma_j^N} \right|^2 P_q(x,Q) \times \left[1 + \mathcal{O}\left(\alpha_s(k_x^2), 1/Q \right) \right] \quad . \tag{4.1}$$

The powers of α_s and (1-x) reflect the behavior of the hard-scattering amplitude at the off-shell value $k_x^2 = \left(\langle k_\perp^2 \rangle + \mathcal{M}^2\right)/(1-x)$ where $\langle k_\perp^2 \rangle$ is set by the spectator transverse momentum integrations. The anomalous dimensions γ_j^N are the anomalous dimensions of the nucleon's valence Fock state wavefunction at

short distances. Their contribution to $G_{q/p}(x,Q)$ are due to the evolution of the wavefunction integrated up to the transverse momentum scale $\ell_\perp^2 < k_x^2$ as in the corresponding exclusive channel analyses. The last factor $P_q(x,Q)$ represents the target-independent evolution of the structure function due to gluon emission from the struck quark: $(C_F = 4/3)$

$$P_q(x,Q) \sim (1-x)^{4C_F\xi(Q)} \tag{4.2}$$

where

$$\xi(Q) = \int_{Q_C^2}^{Q^2} \frac{dj_\perp^2}{j_\perp^2}\, a_s(j^2) \sim \log\left(\frac{\log Q^2/\Lambda^2}{\log Q_0^2/\Lambda^2}\right) . \tag{4.3}$$

The lower limit Q_0^2 of the gluon's transverse momentum integration is set by the mean value of the spectator quark's transverse momenta and masses. This hadronic scale sets the starting point for structure functions evolutions. Equation (4.1) then gives the light-cone momentum distribution for parallel-helicity quarks with x near 1 at the transverse momentum scale Q.

It should be emphasized that the actual momentum scale probed by various deep inelastic inclusive reactions depends in detail on the process under consideration; the actual upper limit of the transverse momentum integration is set by kinematics. For example, if we consider the contribution of Fig. 8 to the deep inelastic structure functions, the propagator (or energy denominator) associated with the top loop reduces to the usual Bjorken structure

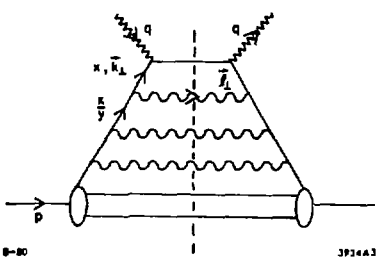

Fig. 8. Perturbative QCD diagrams for structure function evolution.

$2q\cdot p - Q^2/x + i\epsilon$ only if $k_\perp^2 \ll (1-y)Q^2 \leq (1-x)Q^2$ where $k_\perp$ is the quark's transverse momentum and $y \geq x$ is the light-cone variable indicated in the figure. The remaining structure factorizes into a form which defines $G_{q/p}(x/y,k_\perp)$. Thus the actual relation between the structure function and the momentum distribution for $x \sim 1$ is [6,29,30]

$$F_2(x,Q) = \sum_i e_i^2 x_{B_j}\left[G_{q_i/p}(x_{B_j},Q) + \delta G_{q_i/p}(x_{B_j},Q)\right] \qquad (4.4)$$

where

$$\delta G_{q/p}(x,Q) = -2C_F \int_0^1 dy\ \frac{1+y^2}{1-y} \int_{(1-y)Q^2}^{Q^2} \frac{dk_\perp^2}{k_\perp^2}\ \frac{\alpha_s(k_\perp^2/y)}{4\pi}$$

$$\times \left\{G_{q/p}(x/y,k_\perp)\ \frac{\theta(y>x)}{y} - G_{q/p}(x,k_\perp)\right\} \qquad (4.5)$$

corrects for the fact that the top loop is integrated to $k_\perp^2 < (1-y)Q^2$ ($\leq x_{B_j}W^2$) not Q^2. [The argument of α_s is also crucial here.] Other inclusive reactions have to be individually examined: in the case of the Drell-Yan process $q_a\bar{q}_b \to \mu^+\mu^-$, the structure functions evolve to $(1-y_a)Q^2$ and $(1-y_b)Q^2$ not $Q^2 = (p_+ + p_-)^2$.

The actual evolution of structure functions in deep inealstic lepton scattering is thus controlled by the available energy $x_{B_j}W^2$, and is more moderate at $x_{B_j} \sim 1$ than would be expected from lowest order expectations. Analytic forms for the $(1-x)$ behavior are readily computed [29]. The most important features are the following: (1) The $\delta G/G$ correction to leading order in α_s reproduces the critical $2C_F\left(\alpha_s(Q^2)/4\pi\right)\log^2 n$ terms in the structure function moments as calculated using the operator product expansion and renormalization group. In our analysis a series of terms of all orders in $\left(\alpha_s \log^2(1/1-x)\right)^p$ or $\left(\alpha_s \log^2 n\right)^p$ arises simply from the fact that the natural evolution parameter for the structure functions $F_i(x,Q)$ and moments $\mathcal{M}_n(x,Q)$ is controlled by $(1-y)Q^2 < (1-x)Q^2$ and not Q^2; the basic momentum distributions $G(x,Q)$ do not contain the anomalous double-log terms and have a

straightforward perturbative evolution. (2) The extended evolution equations based on Eqs. (4.4) and (4.5) have a number of phenomenological advantages. After taking into account the appropriate evolution limits, each deep inelastic process can be related to the basic distribution $G_q(x,Q)$, avoiding large kinematic corrections. The scale parameter Λ_n which has been introduced to eliminate the strong n-dependent of the higher order corrections to the moments is unnecessary. The fact that xW^2 controls the evolution suggest its use in structure function parameterizations and studies of moment factorization in fragmentation processes. (A study of the application of this method to photon structure functions is in progress.) (3) The exclusive-inclusive connection fails in QCD [29,31]. At fixed but large W^2, $F_{2N}(x,Q)$ falls as $(1-x)^{3+\delta}$ where $\delta > 0$, whereas, modulo logarithmic factors, exclusive channels in QCD give contributions $\sim(1-x)^3$ from the Q^{-4} scaling of the leading nucleon form factors. Thus exclusive channels will eventually dominate the leading twist contributions to inclusive cross sections at fixed W^2, $Q^2 \to \infty$.

A complete treatment of the hadron structure functions must take into account higher twist contributions. Although such contributions are suppressed by powers of $1/Q^2$, they can have fewer powers of $(1-x)$ and, accordingly, may be phenomenologically important in the large x domain [17,32]. In the case of nucleons, the $\ell + qq \to \ell' + qq$ subprocess (in which the lepton recoils against two quarks) is expected to lead to a contribution $\sim(1-x)/Q^4$ since only one quark spectator is required. A large longitudinal structure function is also expected [32,33,34]. Although complete calculations of such terms have not been done, the presence of such terms can reduce the amount of logarithmic scale-violation required from the leading twist contributions in phenomenological fits [32,35].

The analysis of meson structure functions at $x \sim 1$ is similar to that of the baryon, with two striking differneces: (1) The controlling power behavior of the leading twist contribution is $(1-x)^2$ from perturbative QCD [24,36].

The extra factor of (1-x) -- compared to what would have been expected from spectator counting -- can be attributed to the mismatch between the quark spin and that of the meson. (2) The longitudinal meson structure function has an anomalous non-scaling component [33,37] which is finite at $x \to 1$: $F_L(x,Q) \sim Cx^2/Q^2$. This high twist term, which comes from the lepton scattering off an instantaneous fermion-line in light-cone perturbation theory, can be rigorously computed and normalized in perturbative QCD. The crucial fact is that the wavefunction evolution and spectator transverse momentum integrations in Fig. 9 can be written directly in terms of a corresponding calculation of the meson form factor. The result for the pion structure function to leading order in $\alpha_s(k_x^2)$ and $\alpha_s(Q^2)$ is [37,38]

$$F_L^\pi(x,Q) = \frac{2x^2}{Q^2} C_F \int_{m^2/(1-x)}^{Q^2} dk^2 \, \alpha_s(k^2) \, F_\pi(k^2) \qquad (4.6)$$

which numerically is $F_L \sim x^2/Q^2$ (GeV^2 units).

The dominance of the longitudinal structure functions in the fixed W limit for mesons is an essential prediction of perturbative QCD. Perhaps the most dramatic consequence is in the Drell-Yan process $\pi p \to \ell^+\ell^- X$; one predicts [33] that for fixed pair mass Q, the angular distribution of the ℓ^+ (in the pair rest frame) will change from the conventional $(1+\cos^2\theta_+)$ distribution to $\sin^2(\theta_+)$ for pairs produced at large x_L. A recent analysis of the Chicago-Illinois-Princeton experiment [39] at FNAL appears to confirm the QCD high twist prediction with about the expected normalization, see Fig. 10. Striking evidence for the effect has also been seen in a Gargamelle analysis [40] of the quark fragmentation functions in $\nu p \to \mu^+\mu^- X$. The results yield a quark fragmentation distribution into positive charged hadrons which is consistent with the predicted form: $dN^+/dzdy \sim B(1-z)^2 + (C/Q^2)(1-y)$ where the (1-y) behavior corresponds to a longitudinal structure function. It is also crucial to check that the $e^+e^- \to MX$ cross section becomes purely longi-

tudinal ($\sin^2\theta$) at large z at moderate Q^2. The implications of this high twist contribution for meson production at large p_T will be discussed elsewhere [37].

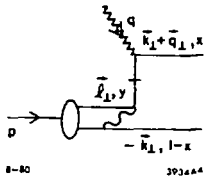

Fig. 9. Perturbative contribution to the meson longitudinal structure function $F_L \sim C/Q^2$.

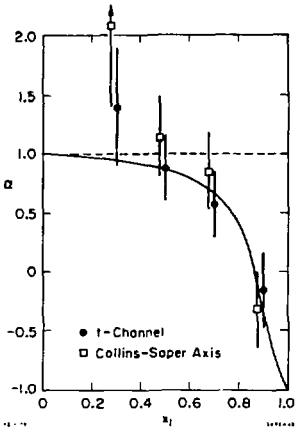

Fig. 10. Comparison of the data of Ref. [39] for the virtual photon polarization in $\pi N \to \mu^+\mu^- X$ with the high twist QCD prediction of Ref. [33]. The μ^+ angular distribution is parametrized as $1+\alpha(x_1)\cos^2\theta_+$ where x_1 is the $\bar{q}$ momentum fraction.

5. Exclusive Processes in QCD: The Two-Photon Processes

As we have emphasized in this talk, the predictions of perturbative quantum chromodynamics can be extended to the whole domain of large momentum transfer exclusive processes. The results lead to a comprehensive new range of rigorous predictions of QCD which test both the scaling and spin properties of quark and gluon interactions at large momentum transfer as well as the detailed structure of hadronic wavefunctions at short distances. The two-photon reactions ($M = \pi, K, \rho, \omega, \ldots$)

$$\frac{d\sigma}{dt}(\gamma\gamma \to M\bar{M}) \qquad \text{at large } s = (k_1+k_2)^2 \text{ and fixed } \theta_{c.m.}$$

provide a particularly important laboratory for testing QCD since these "Compton" processes are, by far, the simplest calculable large-angle exclusive hadronic scattering reactions. As we discuss below, the large-momentum-transfer scaling behavior, the helicity structure, and often even the absolute normalization can be rigorously computed for each two-photon channel [41].

Conversely, the angular dependence of the $\gamma\gamma \to M\bar{M}$ amplitudes can be used to determine the shape of the process-independent meson "distribution amplitudes," $\phi_M(x,Q)$, the basic short-distance wavefunctions which control the valence quark distributions in high momentum transfer exclusive reactions [1,2].

A critically important feature of the $\gamma\gamma \to M\bar{M}$ amplitude is that the contributions of Landshoff pinch singularities are power-law suppressed at the Born level -- even before taking into account Sudakov form factor suppression. There are also no anomalous contributions from the $x \sim 1$ endpoint integration region. Thus, as in the calculation of the meson form factors, each fixed-angle helicity amplitude can be written to leading order in $1/Q$ in the factorized form $\left[Q^2 = p_T^2 = tu/s;\ \tilde{Q}_x = \min(xQ,(1-x)Q)\right]$:

$$\mathcal{M}_{\gamma\gamma \to M\bar{M}} = \int_0^1 dx \int_0^1 dy\ \phi_{\bar{M}}(y,\tilde{Q}_y)\, T_H(x,y,s,\theta_{c.m.})\, \phi_M(x,\tilde{Q}_x) \qquad (5.1)$$

where T_H is the hard-scattering amplitude $\gamma\gamma \to (q\bar{q})(q\bar{q})$ for the production of the valence quarks collinear with each meson (see Fig. 11), and $\phi_M(x,Q)$ is the (process-independent) distribution amplitude for finding the valence q and $\bar{q}$ with light-cone fractions of the meson's momentum, integrated over transverse momenta $k_\perp < Q$. The contributions of nonvalence Fock states are power-law suppressed. Further, the spin-selection rules of QCD predict that vector mesons M and $\bar{M}$ are produced with opposite helicities to leading order in $1/Q$ and all orders in $\alpha_s(Q^2)$.

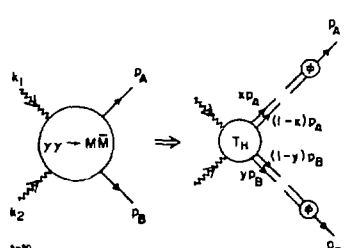

Fig. 11. Factorization of the $\gamma\gamma \to M\bar{M}$ amplitude.

Detailed predictions for each $\gamma\gamma \to M\bar{M}$ helicity amplitude can be worked out to leading order in $\alpha_s(Q^2)$ from the seven diagrams for T_H shown in Fig. 12. The general result is

$$\mathcal{M}_{\gamma\gamma \to M\bar{M}}(s,\theta_{c.m.}) = \frac{\alpha\alpha_s(Q^2)}{Q^2} \sum_{n,m} a_{nm}(\theta_{c.m.}) \left(\ell n\, Q^2/\Lambda^2\right)^{-\gamma_n-\gamma_m} \times \left[1 + \mathcal{O}\left(\alpha_s(Q^2), m/Q\right)\right] \qquad (5.2)$$

where the first factor follows from the fixed angle scaling of T_H. The γ_n are the universal logarithm anomalous dimensions for helicity 0 or helicity 1 mesons as derived from the operator product expansion at short distances [13], or equivalently, the QCD evolution equation for $\phi_M(x,Q)$. Modulo logarithmic corrections, Eq. (5.2) implies $s^4\, d\sigma/dt\,(\gamma\gamma \to M\bar{M})$ scaling at fixed $\theta_{c.m.}$.

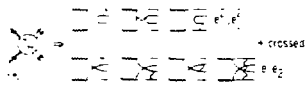

Fig. 12. Leading order contributions to the hard-scattering amplitude T_H.

The QCD predictions for $\gamma\gamma \to \pi^+\pi^-$ and $\gamma\gamma \to \pi^0\pi^0$ to leading order in $\alpha_s(Q^2)$ are shown in Fig. 13. For asymptotic Q^2, $\phi_\pi(x,Q) \Longrightarrow \sqrt{3}\, f_\pi x(1-x)$ and the

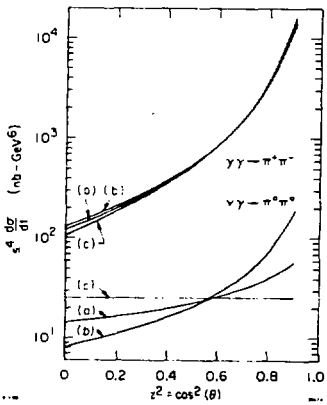

Fig. 13. Perturbative QCD predictions for $\gamma\gamma \to \pi\pi$ at large momentum transfer. Predictions for other helicity-zero mesons only differ in normalization. The curves (a),(b) and (c) correspond to the three distribution amplitudes described in the text.

predictions [curve (a)] become exact and parameter-free. For subasymptotic Q^2, $\phi_\pi(x,Q)$ depends on the details of hadronic binding. Curves (b) and (c) correspond to the extreme examples $\phi \propto [x(1-x)]^{\frac{1}{4}}$ and $\phi \propto \delta(x-\frac{1}{2})$, respectively. In each case it is convenient to rescale the results in terms of the measured pion form factor.

The prediction for other helicity-zero mesons are identical up to overall normalization factors:

$$\mathcal{M}_{\gamma\gamma\to\pi\pi} : \mathcal{M}_{\gamma\gamma\to K\bar{K}} : \mathcal{M}_{\gamma\gamma\to\rho_L\bar{\rho}_L}$$

$$\propto \quad f_\pi^2 \quad : \quad f_K^2 \quad : \quad 2f_\rho^2$$

$$\propto \quad 1 \quad : \quad \sim 1.5 \quad : \quad \sim 2.5 \qquad . \qquad (5.3)$$

For comparison, $s^2\, d\sigma/dt\,(\gamma\gamma \to \mu^+\mu^-) \cong 4\pi\alpha^2(1+z^2)/(1-z^2) \cong 260$ nb GeV^4 at $z \equiv \cos\theta_{c.m.} = 0$.

We note that the $\gamma\gamma \to \pi^+\pi^-$ cross section is insensitive to the shape of $\phi_\pi(x,Q)$. However, because of its different charge structure, the $\gamma\gamma \to \pi^o\pi^o$ amplitude is strongly sensitive to the distribution amplitude: in fact, the $z = \cos\theta_{c.m.}$ dependence of $\mathcal{M}_{\gamma\gamma\to\pi^o\pi^o}$ resolves the x-dependence of $\phi_\pi(x,Q)$ in the same way that the x_{Bj}-dependence of the structure functions. The strong coupling of the x, y, and $\cos\theta_{c.m.}$ variables in $\mathcal{M}_{\gamma\gamma\to M\bar{M}}$ can be traced to the gluon propagators in the last two diagrams for T_H shown in Fig. 12.

We have also computed the cross section for transversely polarized vector mesons with opposite helicity, such as $\gamma\gamma \to \rho_T\bar{\rho}_T$. The predictions in Fig. 14 assume $\phi_\rho(x,Q) = \sqrt{2}(f_\rho/f_\pi)\phi_\pi(x,Q)$ independent of ρ-helicity (although this cannot be strictly true at asymptotic Q^2). The $\gamma\gamma \to \rho_T^o\rho_T^o$ rate vanishes for $\phi_\rho \propto \delta(x-\frac{1}{2})$. We also note that the predicted cross section for $\gamma\gamma \to \rho^+\rho^-$ (summed over polarization) is quite large:

$$\frac{d\sigma/dt\ (\gamma\gamma \to \rho^+\rho^-)}{d\sigma/dt\ (\gamma\gamma \to \mu^+\mu^-)} \sim 7\ \text{GeV}^4/s^2 \qquad (5.4)$$

at $\theta_{c.m.} = \pi/2$.

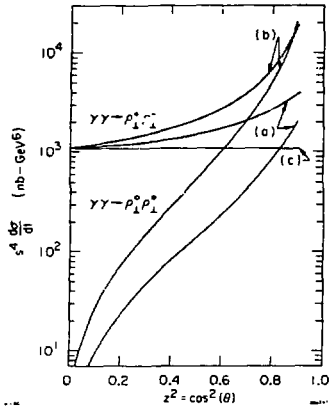

Fig. 14. Perturbative QCD prediction for $\gamma\gamma \to \rho_T\rho_T$ at large momentum transfer, corresponding to the normalization and choices of ϕ_ρ described in the text.

In summary, we note that $\gamma\gamma \to M\bar{M}$ processes can provide a detailed check of the basic Born structure of QCD: the scaling of quark and gluon propagators and interactions, as well as the constituent charges and spin. The form of the predictions are exact to leading order in $\alpha_s(Q^2)$. Power-law (m/Q) corrections can arise from mass insertions, higher Fock states, pinch singularities and non-perturbative effects.

The most extraordinary feature of these results is the fact that the angular dependence of some of the two-photon reactions can directly determine the form of the hadronic wavefunctions at short distances. The determination of $\phi_M(x,Q)$ will remove a major ambiguity in the prediction of the meson form factor. The extension of the results to the baryon channels $\gamma\gamma \to B\bar{B}$ and $\gamma B \to \gamma B$ is thus of obvious interest. The results presented here can also be used to study the occurrence of the fixed Regge singularity at $J = 0$, and the analytic connections to traditional hadronic phenomena: vector meson dominance, finite energy sum rules, and the low energy behavior of the $\gamma\gamma \to M\bar{M}$ amplitudes.

6. Contrasts Between QCD and Parton Model Dynamics

The property of asymptotic freedom in QCD justifies the applicability of many parton model [42] concepts in hadron dynamics. In addition, the Fock state description of hadrons defined at equal time on the light-cone (see Sect. 2) provides a convenient parton-like interpretation of hadron wavefunctions and structure functions at infinite momentum. On the other hand, QCD gives a new perspective into hadron dynamics which is often in direct contradiction to what had been expected in parton or multiperipheral model descriptions. As a summary to this talk we shall list some of these distinguishing characteristics of QCD:

(1) Hadron states of definite particle (quark and gluon) number exist at infinite momentum or at equal time on the light-cone [1]. This is a special consequence of the color neutrality of hadrons; it is not true for particles carrying a gauged current. As we have discussed in Sect. 2, the probability of finding a pion in its $|q\bar{q}\rangle$ valence state can be calculated [3] from its $\pi \to \mu\nu$ and $\pi \to \gamma\gamma$ decay rates. The valence probability is ~1/5 to 1/4.

(2) Exclusive processes at large momentum transfer such as form factors are dominated by hard-scattering subprocesses involving the valence quarks in the hadron's minimum Fock state. The hard-scattering amplitude is then convoluted with the hadron wavefunction evaluated at short distances. This is in striking contrast to parton model mechanisms based on the scattering of a leading quark at $x \sim 1$ in a Fock state with an arbitrary number of wee spectators. As we have emphasized in Sect. 4, the endpoint $x \sim 1$ contributions are always suppressed by the quark Sudakov form factor, relative to the leading hard-scattering contributions. [In the case of helicity zero meson form factors and $\gamma\gamma \to M\bar{M}$ large momentum transfer two-photon processes, the endpoint regions are suppressed by additional kinematic powers of m/Q.] Because of this suppression, the parton model exclusive-inclusive connection fails in QCD. We emphasize that the power-law scaling [43] and helicity dependence of the hard-scattering contributions in exclusive reactions reflect the basic scale-

invariance and spin structure of QCD at short distances. The QCD helicity selection rules [1,2] (see Sect. 3) provide crucial tests of gluon and quark spin.

(3) The leading power-law behavior of inclusive structure functions [1,6,24,25,43] at x near 1 is controlled by the minimum valence Fock state components of the hadron wavefunctions, again in contrast to parton model expectation. The perturbative QCD predictions reflect the elementary scaling of quark and gluon propagators in the far-off shell domain. A striking QCD prediction is that the helicity of the hadron tends to be carried by the constituent with the highest x.

(4) The Fock state structure of QCD at infinite momentum is more complex than usually assumed in phenomenological applications. In addition to the "extrinsic" gluons generated by QCD evolution, there are always "intrinsic" gluons and non-valence quark components in the hadron wavefunction which are insensitive to the momentum scale of the probe [44]. For example, transverse gluons exchanged between quarks, boosted to infinite momentum, yield an intrinsic gluon component to the Fock states. An even more striking example is the prediction [45] of "intrinsic charm" in the proton and meson wavefunctions. One can estimate [46], using the bag model and perturbative QCD, that the proton bound state has a $|uudc\bar{c}\rangle$ component with a probability of ~1-2%. When this state is Lorentz boosted to infinite momentum, the constituents with the largest mass have the highest x. Thus heavy quarks (though rare) carry most of the momentum in the Fock state in which they are present. The usual parton model assumption that non-valence sea quarks are always found at low x is incorrect. The diffractive disassociation of the proton's intrinsic charm state provides a simple explanation why charmed baryons and charmed mesons which contain no valence quarks in common with the proton are diffractively produced at large x_L with sizeable cross sections at ISR energies [47].

(5) It is also interesting to note that nuclear Fock states are much richer in QCD than they would be in a theory in which the only degrees of freedom are hadrons. For example, if we assume that at low relative momentum a deuteron is dominated by its usual n-p configuration, quark-quark scattering automatically generates color-polarized 6-quark states such as $|(uuu)_8(ddd)_8\rangle$ at short distances. The implications of QCD for large momentum transfer nuclear form factors and the nuclear force at short distances is discussed in Ref. [48].

(6) As we have discussed in Sect. 1, the naive procedure of smearing leading twist quark and gluon cross sections with probabilistic parton distributions $G(x,\vec{k}_\perp)$ is incorrect in QCD. The correct procedure for incorporating the effects of wavefunction transverse momenta requires a hard-scattering expansion [12] over higher twist subprocesses. The constituent interchange model [49] represents a first attempt to model such contributions; it is, however, incomplete since only a subset of QCD higher twist diagrams (those with quark exchange or interchange) is included.

(7) The existence of many higher twist contributions in QCD inclusive reactions is a direct consequence of the composite structure of the interacting hadrons. Although they complicate many QCD analyses, particularly hadron production at large transverse momentum, higher twist processes are at the heart of QCD dynamics. In the case of the meson structure function, QCD predicts [25,27,33] a (longitudinal) component $F_L \sim C/Q^2$ which dominates $x \sim 1$ quark distributions and $z \sim 1$ fragmentation phenomena. As we have discussed in Sect. 4, this higher twist term can be absolutely normalized [6] in terms of the form factor scale. We are thus led to critical tests for QCD which are in direct contradiction to parton model predictions. Recent experimental evidence [39,40], in fact, supports the QCD higher twist predictions for the pion structure and fragmentation functions.

(8) Some of the most important tests of QCD involve real photons. In contrast to vector-meson dominance ideas, point-like interactions are predicted to dominate the hadronic interactions of on-shell photons in large momentum transfer reactions [51]. This feature is particularly clear in the QCD predictions for the two-photon inclusive [52] and exclusive processes [5] $\gamma\gamma \to \text{jet} + \text{jet}$ and $\gamma\gamma \to M\bar{M}$, and the photon structure function at large momentum transfer. Higher twist terms should be relatively less important in photon reactions compared to hadron reactions.

(9) The generation of hadron multiplicity is not completely understood in QCD. However a number of features are anticipated which appear to differ strongly from parton model expectations: For example, in QCD (a) the final state multiplicity reflects the color separation set up in the collision [53]; this is believed to even hold in low p_T hadron collisions since the basic interactions involve color exchange; (b) the evolution in space-time corresponds to an inside-outside cascade -- the slowest hadrons are created first; (c) the final state multiplicity in the Drell-Yan process $AB \to \ell\bar{\ell}X$ is expected to reflect the creation of 3_c and 3_c^- spectator systems at the moment of annihilation [53]; and (d) the multiplicity of gluon jets and other color octet systems should reflect its higher color charge relative to color triplet systems [53]. It is clear that QCD provides a novel perspective for multiparticle phenomena.

(10) Another critical testing ground of QCD dynamics is the study of quark and gluon interactions in nuclear targets [55]. For example, consider the Drell-Yan process $\bar{p}U \to \mu^+\mu^- X$. If the factorization theorem for inclusive reactions is correct the cross section at large pair mass Q is given by the convolution of the anti-proton structure function $G_{\bar{q}/\bar{p}}(x_a,Q)$ with the nuclear distribution function $G_{q/U}(x_b,Q)$ -- which for large Q^2 is $\sim A G_{q/N}(x_b,Q)$. Thus the factorization theorem predicts no absorption of the constituents of the anti-proton despite the fact that the $\bar{p}$ suffers repeated inelastic collisions in its passage through the nuclear volume! If this is really

correct, then only wee quarks and gluons with $x \sim 0$ (finite momentum in the lab frame) can be strongly absorbed; the nucleus is then essentially transparent to the valence Fock state of the hadron.

From a physical point of view, it seems much more reasonable that an incident hadron's Fock state will be strongly altered because of Glauber inelastic collisions during its passage through the nucleus [56]. Standard QCD evolution then applies to the altered structure function -- i.e., the "initial conditions" are not the same as in deep inelastic lepton scattering. This is of course in contradiction to the QCD factorization theorem. We also expect that the effects of nucleon absorption and collisions will be strongest for those Fock components of the incident hadron which are largest in transverse spatial extent, i.e., Fock states with a high multiplicity of wee quarks. The nucleus then acts as a differential absorber where the valence Fock state (and hence quarks with large x) suffer the least absorption. The crucial test of this idea is the A-dependence of the Drell-Yan cross section $pA \to \mu^+\mu^- X$ as a function of the momentum fraction x_a of the annihilating antiquark, to see whether nuclear absorption sets in at $x \lesssim \hat{x}$ where $\hat{x}$ is fixed or vanishes with increasing momentum as required by the factorization theorem [57].

ACKNOWLEDGEMENTS

Part of the work presented here is based on collaborations with E. Berger, Y. Frishman, T. Huang, C. Sachrajda, and S. A. A. Zaidi. Portions of the talk were also presented at the XXth International Conference on High Energy Physics, Madison, Wisconsin (1980), in SLAC-PUBs 2587 and 2601.

REFERENCES

1. Brodsky, S. J. and Lepage, G. P. (SLAC-PUB-2294), published in "Quantum Chromodynamics," Proceedings of the 1978, La Jolla Institute, W. Frazer and F. Henyey, eds., AIP, 1979; Lepage, G. P. and Brodsky, S. J., Phys. Lett. 87B, 359 (1979), Phys. Rev. Lett. 43, 545 (1979), Erratum ibid 43, 1625 (1979); Brodsky, S. J., Frishman, Y., Lepage, G. P. and Sachrajda, C., Phys. Lett. 91B, 239 (1980); Brodsky, S. J. and Lepage, G. P. (SLAC-PUB-2447), published in the 1979 Summer Institute on Particle Physics at SLAC, Stanford, California.

2. Lepage, G. P. and Brodsky, S. J., SLAC-PUB-2478 (1980), to be published in Phys. Rev. D.

3. Brodsky, S. J., Huang, T. and Lepage, G. P., SLAC-PUB-2540 (1980), Contributed to the XXth International Conference on High Energy Physics, Madison, Wisconsin, July 17-23, 1980; Huang, T., SLAC-PUB-2580 (1980), to be appeared in Proceedings of Madison Conference.

4. Brodsky, S. J., Lepage, G. P. and Zaidi, S. A. A., SLAC-PUB-2588 (1980).

5. Brodsky, S. J. and Lepage, G. P., SLAC-PUB-2587 (1980), to be appeared in Proceedings of the XXth International Conference on High Energy Physics, Madison, Wisconsin, July 17-23, 1980.

6. Brodsky, S. J. and Lepage, G. P., SLAC-PUB-2601 (1980), to be appeared in Proceedings of the XXth International Conference on High Energy Physics, Madison, Wisconsin, July 17-23, 1980.

7. See Buras, A. J., Rev. of Mod. Phys., Vol. 52, No. 1, January 1980, p. 199, and references therein.

8. Efremov, A. V. and Radyushkin, A. V., Dubna preprints JINR-E2-11535, 11983 and 12384.

9. Duncan, A. and Mueller, A. H., Phys. Lett. 90B, 159 (1980), Phys. Rev. D21, 1636 (1980); Duncan, A., Symposium on Topical Questions in QCD, Copenhagen, 1980; Mueller, A., the XIth International Symposium on Multiparticle Dynamics, Bruges, Beglium, June 22-27, 1980.

10. The $Q^2 \to \infty$ asymptotic result for the pion form factor was first obtained by Farrar, G. R. and Jackson, D. R., Phys. Rev. Lett. 43, 246 (1979); see also Chernyak, V. L. and Zhitniskii, A. R., JETP Lett. 25, 11 (1977).

11. The rules for light-cone perturbation theory, or equivalently time-ordered perturbation theory in the infinite momentum frame, and references to earlier work are given in Ref. 2.

12. Brodsky, S. J., Caswell, W. E. and Horgan, R. R., Phys. Rev. D18, 2415 (1978); Politzer, H. D., Caltech preprints 68-765 and 68-789, presented at the *Symposium on Topical Questions in QCD*, Copenhagen, 1980.

13. An operator product analysis of hadronic wavefunctions at short distances is given in Brodsky, S. J., Frishman, Y., Lepage, G. P. and Sachrajda, C., Ref. 1. See also Efremov, A. V. and Radyushkin, A. V., Ref. 8. The baryon wavefunction anomalous dimensions derived in Refs. 1 and 2 have been confirmed by Peskin, M., Phys. Lett. 88B, 128 (1979).

14. Drell, S. D. and Yan, T. M., Phys. Rev. Lett. 24, 181 (1970); West, G., Phys. Rev. Lett. 24, 1206 (1970).

15. Lipatov, L. N., Yad. Fiz. 20, 181 (1974) [Sov. J. Nucl. Phys. 20, 94 (1974)]; Altarelli, G. and Parisi, G., Nucl. Phys. B126, 298 (1977).

16. See Berger, E. L. and Brodsky, S. J., Phys. Rev. Lett. 42, 940 (1979); Farrar, G. R. and Jackson, D. R., Ref. 26; Berger, E., Brodsky, S. J. and Lepage, G. P., in preparation.

17. For phenomenological applications of high twist subprocesses, see, e.g., Blankenbecler, R., Brodsky, S. J. and Gunion, J. F., Phys. Rev. D18, 900 (1978); Blankenbecler, R. and Schmidt, I., Phys. Rev. D16, 1318 (1977); Abbott, L., Atwood, W. and Barnett, R. M., Phys. Rev. D22, 582 (1980), and references therein.

18. Schwinger, J., Phys. Rev. 82, 664 (1951); Adler, S. L., Phys. Rev. 177, 2426 (1969); Bell, J. S. and Jackiw, R., Nuovo Cimento 60A, 47 (1969).

19. Jackiw, R., in "Lectures on Current Algebra and Its Applications," Princeton University Press, pp. 97-230. We are grateful to Frishman, Y. for discussions on this problem.

20. See, for example, Elementary Particle Theory Group, Beijing University, Acta Physics Sinica 25, 415 (1976).

21. Karmanov, V. A., ITEP-8, Moscow, 1980.

22. De Rujula, A. and Martin, F., CTP 851, MIT preprint, 1980.

23. Brodsky, S. J. and Blankenbecler, R., Phys. Rev. D10, 2973 (1974).

24. Ezawa, Z. F., Nuovo Cimento 23A, 271 (1974).

25. Farrar, G. R. and Jackson, D. R., Phys. Rev. Lett. 35, 1416 (1975).

26. The data are from the analysis of electroproduction $e^- p \to e^- + \pi^+ + n$; Bebek, C. et al., Phys. Rev. D13, 25 (1976).

27. See also Vainshtain, A. I. and Zakharov, V. I., Phys. Lett. 72B, 368 (1978); Farrar, G. R. and Jackson, D. R., Ref. 25.

28. The data are from: Mestayer, M. D., SLAC Report 214 (1978) and references therein.

29. Brodsky, S. J. and Lepage, G. P., SLAC-PUB-2447 (1979), published in 1979 Summer Institute on Particle Physics at SLAC, Stanford, California.

30. See also Curci, G. and Greco, M., Phys. Lett. 92B, 175 (1980); Amati, D. et al., CERN-TH-2831 (1980); Ciafaloni, M., the XXth International Conference on High Energy Physics, Madison, Wisconsin, July 17-23, 1980.

31. See also Parisi, G., Phys. Lett. 84B, 225 (1979).

32. Blankenbecler, R. and Schmidt, I., Phys. Rev. D16, 1318 (1977); Blankenbecler, R., Brodsky, S. J. and Gunion, J. F., Phys. Rev. D12, 3469 (1975).

33. Berger, E. L. and Brodsky, S. J., Phys. Rev. Lett. 42, 940 (1979); Berger, E. L., Phys. Lett. 89B, 241 (1980).

34. Abbott, L. et al., Phys. Lett. 88B, 157 (1979).

35. Abbott, L. et al., Ref. 17.

36. This result assumes the mass of the spectator is finite. If $\mathcal{M} \to 0$, perturbative and even non-perturbative calculations allow $F_{2\pi}(x) \sim (1-x)$. See De Rujula, A and Martin, F., Ref. 22; Brodsky, S. J. et al., Ref. 3.

37. Tests of this result will be discussed in Berger, E. L., Brodsky, S. J. and Lepage, G. P., in preparation.

38. See also Duncan, A. and Mueller, A., Phys. Lett. 90B, 159 (1980).

39. Anderson, K. J. et al., Phys. Rev. Lett. 43, 1219 (1979).

40. CERN-MILAN-ORSAY Collaboration, CERN-EP/80-124 (1980); Matteuzzi C. et al., Contributed to the XXth International Conference on High Energy Physics, Madison, Wisconsin, July 17-23, 1980.

41. Complete results will be given in Brodsky, S. J. and Lepage, G. P., in preparation.

42. Feynman, R. P., Photon-Hadron Interactions, W. A. Benjamin (1972).

43. Brodsky, S. J. and Farrar, G. R., Phys. Rev. Lett. 31, 1153 (1973), Phys. Rev. D11, 1309 (1975); Matveev, V. A., Muradyan, R. M. and Tavkhelidze, A. V., Lett. Nuovo Cimento 7, 719 (1973).

44. Brodsky, S. J. and Gunion, J. F., Phys. Rev. D19, 1005 (1979).

45. Brodsky, S. J., Hoyer, P., Peterson, C. and Sakai, N., Phys. Lett. 93B, 451 (1980).

46. Donoghue, J. F. and Golowich, E., Phys. Rev. D15, 3421 (1977).

47. For a review see the rappateur talk of Phillips, R., the XXth International Conference on High Energy Physics, Madison, Wisconsin, July 17-23, 1980.

48. Brodsky, S. J. and Lepage, G. P., SLAC-PUB-2595, to be published in the Proceedings of the IXth International Conference on the Few Body Problem, Eugene, Oregon, 1980; Brodsky, S. J. and Chertok, B. T., Phys. Rev. Lett. 37, 279 (1976) and Phys. Rev. D14, 3003 (1976).

49. Blankenbecler, R. et al., Ref. 17.

50. See, e.g., Rückl, R., Brodsky, S. J. and Gunion, J. F., Phys. Rev. D18, 2469 (1978); Horgan, R. and Scharbach, P., CERN preprint (1980).

51. See, e.g., Brodsky, S. J., Close, F. E. and Gunion, J. F., Phys. Rev. D6, 177 (1972).

52. See, e.g., Brodsky, S. J., DeGrand, T. A., Gunion, J. F. and Weis, J. H., Phys. Rev. D19, 1418 (1979).

53. Brodsky, S. J. and Gunion, J. F., Phys. Rev. Lett. 37, 402 (1976). See also the talks of Gunion, J. F. and Capella, A., Proceedings of the XIth International Symposium on Multiparticle Dynamics, Bruges, Belgium, 1980.

54. Kogut, J. and Susskind, L., Phys. Rev. D10, 732 (1974); Bjorken, J., in Lecture Notes in Physics, "Current-Induced Reactions," Springer-Verlas (N.Y.), 1975.

55. See, e.g., the contributions of Biatas, A. and Brodsky, S. J., in the Proceedings of the 1st Workshop on Ultra-Relativistic Nuclear Collisions, Berkeley, California, 1979.

56. Brodsky, S. J. and Lepage, G. P., to be published.

57. Gupta, S. and Mueller, A., Phys. Rev. D20, 118 (1979), and references therein. We also wish to thank A. Mueller and S. Gupta for discussions.